Surface Modification of
Indium Tin Oxide

by

Dongho Kim

B.Sc., University of British Columbia, 2012

Thesis Submitted in Partial Fulfillment of the

Requirements for the Degree of

Master of Science

in the

Department of Chemistry

Faculty of Science

Approval

Name:	**Dongho Kim**
Degree:	**Master of Science**
Title:	***Surface Modification of Indium Tin Oxide***
Examining Committee:	**Chair:** Krzysztof Starosta Associate Professor Graduate Program Chair

Byron Gates
Senior Supervisor
Associate Professor

_____

Michael Eikerling
Supervisor
Professor

_____

Jeffrey Warren
Supervisor
Assistant Professor

_____

Hogan Yu
Internal Examiner
Professor

_____

Date Defended/Approved: July 26, 2017

_____

Abstract

Indium tin oxide serve a critical function in many organic devices, such as organic light emitting diodes and organic photovoltaics. To optimize the performances of these devices, it is desirable to tune the interface between the indium tin oxide and the next functional layer of these devices. A common surface modification of transparent conductive oxides is through the use of self-assembled monolayers. This methodology enables a simultaneously tuning of the properties and performance of this interface, including the surface energy, work function and durability of the transparent conductive oxide. Phosphonic acid and silane based monolayers have been extensively studied and used in devices for their ability to tune the interfacial properties of transparent conductive oxide. Herein, alcohol based monolayers are first demonstrated on transparent conductive oxide surfaces. The electrochemical and chemical stabilities of alcohol based monolayers, as well as changes in the optical properties of the Indium tin oxide as a function of their stability were evaluated in comparison to more traditional routes of surface modification, such as through the use of silanes and phosphonic acid based monolayers. The tunability of both work function and surface energy of the modified Indium tin oxide were also determined for assessing their electronic properties.

Keywords: transparent conductive oxide (TCO), indium tin oxide (ITO), alcohol based monolayers, stability, work function, surface energy

To my beloved family and friends

Acknowledgements

I would like to thank my supervisor, Dr. Byron D. Gates, for the great opportunity to work with him and to gain this valuable experience. I deeply appreciate his guidance and support in my study, as well as for my future.

I would also like to thank my committee members, Dr. Michael Eikerling and Dr. Jeffery Warren, for their critical review of my research and encouragements.

Thanks to Molecular Analysis Facility at University of Washington for access to ultraviolet photoelectron spectroscopy, which was extremely helpful for my degree.

I also want to thank my colleagues for their support and help. I genuinely enjoyed working with them and valuable conversations we had on research and life over a coffee or a beer.

I appreciate the input from Austin Lee and Dr. Jennie Eastcott in my research and assistances from the staffs at SFU and UW (Seattle, WA, USA) during my degree.

Lastly, I thank my family for their continued support in pursuing my academic goals.

Table of Contents

List of Tables

List of Figures

List of Acronyms

ALD	Atomic layer deposition
CA	Contact angle
CBM	Conductive band minimum
CdO	Cadium oxide
CE	Counter electrode
CV	Cyclic voltammetry
DCdiA	1,10-decanediol
E_B	Binding energy
E_F	Fermi level
EIL	Electron injection layer
E_K	Kinetic energy
EML	Emission layer
E_{sec}	Secondary electron cut-off edge
ETL	Electron transport layer
E_{vac}	Vacuum level
HIL	Hole injection layer
HOMO	Highest occupied molecular orbital
HTL	Hole transport layer
IMFP	Inelastic mean free path
ITO	Indium tin oxide
j_{ac}	Activation controlled current
j_{diff}	Diffusion controlled current
$K_3[Fe(CN)_6]$	Potassium ferricyanide
$K_4[Fe(CN)_6]$	Potassium ferrocyanide
LUMO	Lowest unoccupied molecular orbital
ODA	1-octadecanol
ODPA	Octadecylphosphonic acid
ODTS	Octadecyltrichlorosilane
OLED	Organic light emitting diode
OPV	Organic photovoltaic
PFOA	1H,1H,2H,2H-perfluorooctanol
PTdiA	1,5-pentanediol

RCA-1	Radio Corporation of America standard cleaning 1 procedure
RE	Reference electrode
SAMs	Self-assembled monolayers
TCO	Transparent conductive oxide
UPS	Ultraviolet photoelectron spectroscopy
UV-Vis	Ultraviolet-visible spectroscopy
VBM	Valence band maximum
W	Work of adhesion
WCA	Water contact angle
WE	Working electrode
XPS	X-ray photoelectron spectroscopy
Φ	Work function
γ	Surface tension
θ	Contact angle

Glossary

By-Product	Unintended but inevitable product from a chemical reaction
Conduction Band Minimum	Lowest vacancies of electronic states at absolute zero (0 K) in a material
Fermi Level	Highest energy level occupied by electrons at absolute zero (0 K) in a material
Hydrophobicity	Resistance to water
n-type Semiconductor	A type of extrinsic semiconductor, which has been doped with a pentavalent species that can donate an extra electron for conduction
Self-Assembled Monolayers	Spontaneously formed assemblies of molecules as a result of surface energies, reactive surfaces and from intermolecular interactions
Surface Energy	The total intermolecular forces on the surfaces of a material that result in a net attractive or repulsive force when interacting with other materials or molecular species
Vacuum Level	Electronic properties of any material - an energy of a stationary electron outside of a material
Valence Band Maximum	Highest energy level occupied by electrons at absolute zero (0 K) in a material
Work Function	Energy required to pull a single electron from the Fermi level to the vacuum level
Electron Affinity	Energy required or gained through moving an electron from the vacuum level to the conduction band minimum

Chapter 1.

Introduction

1.1. Indium Tin Oxide: Properties and Modifications

1.1.1.   Properties of Indium Tin Oxide

Transparent conductive oxides (TCOs) are semiconductors that have become prevalent in the recent decades because of many applications for these materials in electronic devices. The TCOs are often utilized as anodes in solar panels, heat reflective coatings on windows, touch screens, organic photovoltaics (OPVs), and displays that include organic light emitting diodes (OLEDs) and light emitting diodes (LEDs).[1-7] After the first TCO, cadmium oxide (CdO), was discovered in 1907, multiple types of TCOs were reported and studied extensively.[8] The criteria for TCO are: i) a band gap (E_G) size that is greater than or equal to 3 electron volts (eV) for transparency; ii) a carrier concentration of at least 10^{20} cm^{-3}; and iii) a resistivity less than 10^{-4} ohm/cm.[8] These criteria are the classification of which materials are TCOs with a minimum conductivity and transparency. The most common type of materials used in preparing TCOs are n-type semiconductors, which include indium oxide (In_2O_3), tin oxide (SnO_2), and zin oxide (ZnO) based materials.[6, 8-9] Among these TCOs, indium tin oxide (ITO) has been the standard material for organic electronics because of its high conductivity over a wide range of temperatures, its high degree of transparency in the visible spectrum (~90% transparency when deposited on a glass substrate), and its high work function.

Indium tin oxide (ITO) is an In_2O_3 based n-type semiconductor with tin as a dopant. Indium oxide has a bixbyite unit cell structure, which has two oxygen vacancies.[1] These vacancies result in two free electrons. An additional free extra electron is generated, when In^{3+} is replaced with Sn^{4+}. These free electrons form an energy level just below the conduction band. Currently, commercial ITO targets include 10 mol% Sn. Based on

1

previous studies, at approximately 20 mol% Sn the neutral SnO_2 begins to form.[10] The formation of the SnO_2 species reduces the number of free electrons that contribute to the conductivity. This loss of free electrons leads to an increase in the resistivity of the ITO.

Another interesting aspect of ITO is the band gap size. Some studies have reported sizes of ITO band gap as small as 3 eV, while others have reported band gaps as large as 3.9 eV.[1, 11-13] In order to address the large discrepancies in reported band gap sizes for ITO, the presence of indirect band gap has been suggested in multiple studies.[9, 11, 13] An indirect band gap refers to a non-symmetry in the conduction and valence band structures. The offset of the band structures results in a larger apparent band gap, which gives rise to the optical transparency of these thin films. These properties have led to ITO becoming the standard material among other TCOs for various devices that include touch screens and displays.[6, 8-9, 11]

Besides the conductivity and transparency of TCOs, there is another important criterion for the choice of materials in display devices. The Schottky barrier and surface energy are two main properties that are directly related to device performance. The Schottky barrier is involved with hole injection processes and work function of interfaces within the devices. For example, the brightness of displays depends on the interfacial properties between the TCO and hole transport layer (HTL) or hole injection layer (HIL). This barrier determines the efficiency of electron transport between layers within devices.[14] For these devices, materials with high work function is desired to minimize this barrier. Among TCOs, ITO exhibits a relatively high work function (~4.6 eV).[8]

Despite of these beneficial properties of ITO, some challenges still remain with incorporating ITO into devices, such as into OLEDs and OPVs, mainly due to the degradations of ITO and its surface modifications. Currently, devices that utilize ITO as an anode are faced with the degradation of ITO and its surface modification overtime. Specifically in OLEDs and OPVs, the thermal, electrochemical, and photochemical degradation can lead to compromised device performance and shortening of the device lifetime. Thermal degradation leads to the loss of contact between ITO and the HTL, which impairs the device performance. Electrochemical degradation can take place at the ITO and HTL interface during device operation. This process involves the formation of electronic traps, where electrons cannot be transported to the adjacent layer and charging

is observed at the interface. The photochemical degradation refers to the loss of electroluminescence, which is caused by irradiation of light at energies larger than electronic gap of the semiconducting organic materials. Another challenge is that indium ions can leach into the organic layer that is deposited onto the ITO during device operations. This loss of indium ions also leads to a decrease in the conductivity.[1, 15] Inorganic and organic surface modifications of ITO have been proposed to address these issues. In this thesis, surface modification through the preparation of heteroatom free organic monolayers is pursed to achieve highly stable surface modifications on ITO, as well as to design an interface with the desired electronic properties and long-term stabilities.

1.1.2.   Surface Modifications on Indium Tin Oxide (ITO)

1.1.2.1 Inorganic Surface Modifications of ITO

Multiple solutions have been proposed to prevent and compensate for the degradation of ITO in OLED devices.[1, 12, 16] One approach is modifying the surfaces with a thin metal film through physical deposition techniques. This approach has shown its effectiveness in tuning work function of ITO. For example, thin gold films are already used in commercial systems to improve the performance of organic electronics.[1] The most common metal thin films used to modify the ITO surfaces include Pt, Au, Cu and Ni.[17-20] Thin gold films can successfully minimize the degradation of ITO, can increase the work function up to 5.1 eV and can improve the physical contact with HTL, which enhances the performance and prolongs the lifetime of OLED devices.[17] Some trade-offs, however, exist with inorganic surface modifications. In order to maintain the transparency of the ITO, the film thicknesses must be less than or equal to 0.5 nm.[1] Therefore, this process requires extremely precise and control over the process of film deposition. Due to interfacial tension (e.g., surface tension) of the materials used to form these atomic thin films, these coatings are likely to form nanodots and lead to changes in the surface morphologies. Therefore, these coatings often lack uniformity in the resulting surface morphology. The non-uniformity at the interface limits the ability to tune the surface energy and the work function to localized effects, which leads to large uncertainties when determining the hole injection barrier.

3

Another method to modify the ITO surfaces is through the use of metal oxide films deposited onto the ITO surfaces. This approach provides a few benefits over the use of metal thin films. Transition metals are often used to form a metal oxide films, such as Al_2O_3, MoO_3, WO_3, Ag_2O and Pr_2O_5, which are more transparent than pure metal thin films and induce permanent dipole moments at the interface.[19, 21-23] Studies have shown that OLED devices that utilize metal oxide thin films exhibit a good stability over a wide range of thicknesses. Another benefit is that these thin films can also improve the power efficiency of the electronic devices. For example, an MoO_3 layer can exhibit permanent dipole moments that maximize the work function at this surface (up to 6.3 eV).[23] Approximately 10 times higher hole injections and 2 times higher power efficiencies were observed with the use of Pr_2O_5 in OLED devices.[19] These increases in the device efficiencies were also observed in their overall performance, such as a 60% increase in the luminance observed with the incorporation of Ag_2O thin films.[24]

Similar to metal thin films, metal oxide films are also prepared through deposition techniques that can lead to a non-uniformity of the resulting films, which confines the modified surface properties to localized effects.[1] A variety of organic surface modifications and atomic layer deposition (ALD) techniques were employed to achieve more uniform surface modifications. The ALD technique is, however, very costly to operate, especially on large substrates. As an alternative to inorganic surface modifications, some organic surface modifications have been proposed to tune surface properties of ITO.

1.1.2.2 Organic Surface Modifications of ITO

Organic surface modifications of ITO, unlike inorganic modifications, are often utilized to modify the interfacial chemistry and minimize degradation of the ITO surfaces.[5, 16, 25-33] There are multiple methods to modify the surfaces of ITO with organic materials. These surface modifications are often sought to serve as a support layer for the deposition of organic based functional materials, such as conductive polymers, HTL and HIL used in the preparation of devices based on a multilayer design.[1, 3, 12] Majority of these functional organic materials are often spin coated or drop-cast on the ITO. These materials form relatively thick layers, which are distinguishable from self-assembled monolayers (SAMs) that are covalently bonded to the ITO surfaces and are often used underneath these functional organic films to tune their surface wetting and electronic properties of this interface. In this thesis, the wider deposition of organic materials onto ITO will not be

discussed in detail, but will instead focus on organic surface modifications to prepare SAMs.

Monolayer-based surface modifications have been investigated for their ability to minimize the degradation of ITO and to design an interface with respect to the work function and the surface energy of this interface within an organic electronic device.[5, 12, 16, 25, 27, 29-30, 32-35] To date, this methodology has been demonstrated for its effectiveness to create an interface with desired properties and demonstrated for its compatibility with common HTL materials. Another benefit of this approach is that monolayers enable the simultaneous modifications of the work function and surface energy of ITO. There are primarily two types of organic layers used to modify ITO surfaces: silanes and phosphonic acids. Monolayers derived from carboxylic acids and thiols have also been studied previously.[35] Due to their weak interactions with the oxide surfaces, in comparison to silane and phosphonic acids, they will not be discussed in this work. Both silane and phosphonic acid approaches are currently being utilized in the display industries and have demonstrated their ability to tune surface properties.[36] Figure 1.1 illustrates silane and phosphonic acid based monolayers on ITO surfaces and their theoretical packing density. Although the formations of both of these types of monolayers are dictated by the available hydroxyl groups on native ITO surfaces, silane based monolayers can exhibit a slightly lower packing density due to the orientation of the molecules.[1, 16]

Silanes are one of the commonly used organic monolayers used for modifying ITO surfaces, and are capable of forming covalent bonds (e.g., In-O-Si bonds). Silane based monolayers have a number of advantages that include a relatively short solution reaction time and insensitivity to reaction conditions, such as concentrations of precursors and temperatures of preparing solutions (e.g., room temperature). These SAMs can tune surface properties and forming up to three covalent bonds.[1, 12] Under ambient conditions, silane precursors readily self-polymerize to form a chain over ITO surfaces, which results in a high surface coverage. Furthermore, among all surface modifications to ITO through the use of monolayers, silanes have the shortest reaction time (~ 2 h, compared to ~24 h for phosphonic acid and alcohol based monolayers). Surface modification through the use of silanes have shown promising results that include an increase in the work function of and luminance in OLED devices.[5, 29, 37-40] Using octadecyltrichlorosilane (ODTS) as a precursor, the work function of ITO was increased to 4.85 eV and decreased surface

5
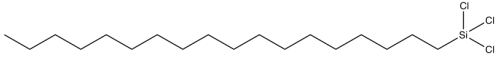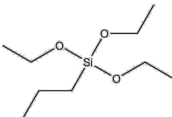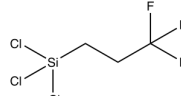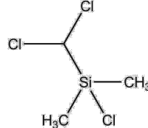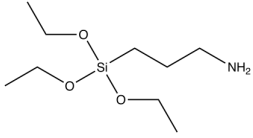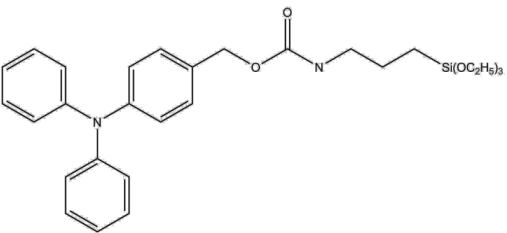
energy to 29.3 mJ m^{-2}. With functionalized terminal groups, the work function and surface energy of the ITO could be further modified to minimize mismatching properties between the ITO and the HTL. For example, [4-(diphenylamino) phenyl]methoxy-*N*-(4,4,4-triethoxy-4-silabutyl)formamide was used to form monolayers on ITO surfaces and investigated improving the OLED device performance.[5] The device characterization resulted in achieving a work function of 5.3 eV and approximately a 2.3-fold increase in brightness without a significant change in the onset potential of the device, although the surface modification increased the work function by ~0.5 eV. This observation was attributed to the increased contact surface area between ITO and the deposited organic layers. Through this surface modification, the surface energy of the ITO was significantly reduced to be compatible with the organic coatings applied to the ITO. This approach allowed these devices to endure higher currents in comparison to unmodified ITO. Another study that utilized a fluorine moiety at the ITO surfaces of the monolayers (3,3,3-trifluoropropyltrichlorosilane) demonstrated 5.16 eV and 28.7 mJ m^{-2} for the work function and surface energy, respectively.[30] Similarly, many studies have demonstrated either an increase in the work function or a decrease in the surface energy to enhance device performance (Table 1.1).
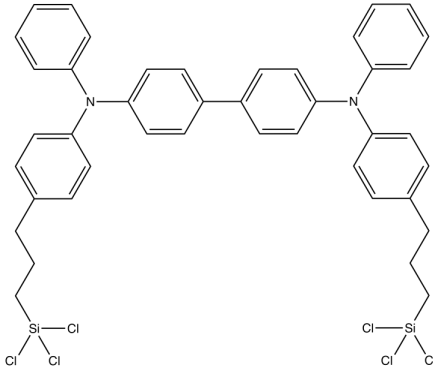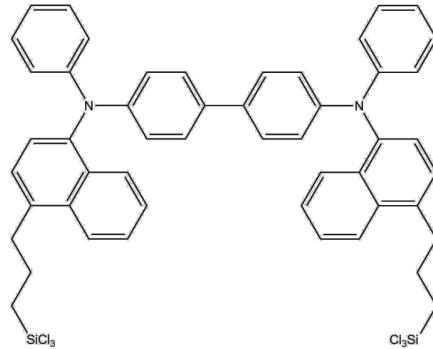
Despite the benefits from silane derived monolayers, there are major drawbacks in the stability under ambient conditions to which include: (i) moisture sensitivity of the precursors; (ii) hydrolytic instability of the monolayers; (iii) limitations to the achievable functional terminal groups, such as hydroxyls, carbonyls and nitryls; and (iv) their susceptibility to form multilayer formation.[1, 41] Silanes are extremely sensitive to moisture as these reagents can undergo condensation reactions to form Si-O-Si bonds in the presence of moisture. Therefore, these reagents often require a controlled environment for handling. Moreover, silane based monolayers have a tendency to degrade when exposed to moisture and heat. Their hydrolytic and thermal instabilities have been reported in multiple studies.[41-43] More importantly, because silanes are extremely reactive towards hydroxyls, carbonyls and nitryls, if any of these functional groups are present within the reagents, silanes can self-polymerize and become non-reactive. Consequently, silanes are restricted to a limited choice of terminal functional groups on precursors.

Another critical issue with silanes is the uniformity of the resulting monolayers. The formation of multilayers could not only reduce the overall induced dipole at the interface

between ITO and monolayers, but also increase the surface roughness.[44] The relationship between surface roughness and wetting have been well known. An increase in surface roughness can result in poorer wetting of the HTL. Therefore, in order for the HTL to be uniformly deposited and be stable, multilayer formations of the monolayers should be avoided when possible.

Table 1.1 **Work functions and surface energies reported for a series of silane surface modifications on ITO.**

chemical structure	work function (eV)	surface energy (mJ/cm^2)	reference
n-octadecyltrichlorosilane	4.85	29.3	28
triethoxy(ethyl)silane	3.87	31.4	29
trichloro(3,3,3-trifluoropropyl)silane	5.16	28.7	29
(dichloromethly)dimethlychlorosilane	0.3*	N/R*	40
aminopropyltriethoxysilane	4.35	46.5	29
TPA-CONH-Si	5.3	N/R*	5

TPD-Si	5.2	N/R*	50
NPB-Si	5.4	N/R*	50

(N/R = not reported in the literature and * = only change reported)
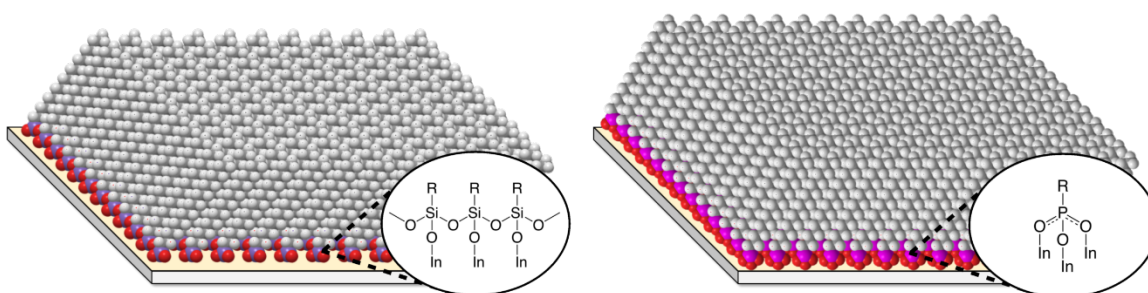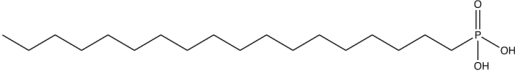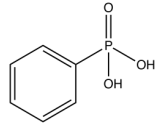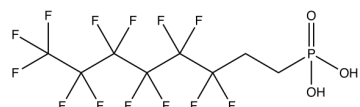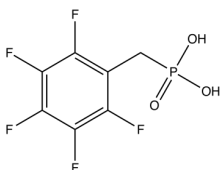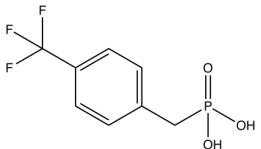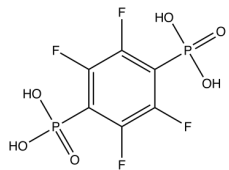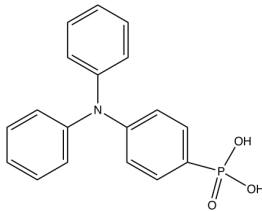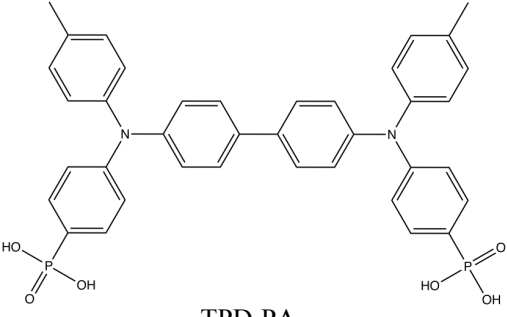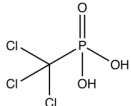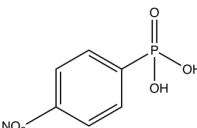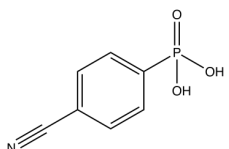
Figure 1.1 **Monolayers prepared from octadecyltrichlorosilane (left) and octadecylphosphonic acid (right), reflecting their packing densities on ITO surfaces.**

Another alternative to inorganic surface modifications to ITO is through the use of phosphonic acid based monolayers. These monolayers form through covalent In-O-P bonds and offer a few advantages over silane based monolayers. The benefits include the formation of a single layer, ease of synthesizing and storing precursors, and availability of

various terminal functional groups (Table 1.2).[1, 7, 12, 25, 28, 45] This type of surface modification also offers up to three covalent bonds, similar to silane based monolayers. However, phosphonic acids can be sensitive to reaction conditions, such as concentrations of reagents and composition and purity of solvents. The solvent can influence the formation of phosphonic based monolayers. Previous studies on solvent effects for the formation of phosphonic acid based monolayers concluded that each precursors requires specific solvents to achieve the high quality monolayers.[46] An additional sintering process is often performed to stabilize the covalent bond, In-O-P, and to achieve high quality monolayers. Previous studies have shown that phosphonic acid based monolayers can tune the work function and surface energy of ITO and prolong the lifetime of OLEDs through the uses of various precursors with different terminal functional groups.[2, 12, 25-28, 34, 47] In the study, different phosphonic acid modifiers, including phenylated and fluorinated molecules, were utilized to form monolayers and were characterized using XPS, UPS, and WCA.[27] The result showed that these monolayers have close to a full surface coverage (86-90%), increased work function by 0.6 eV, and surface energies as low as 24 mJ m^{-2}. Another study demonstrated the tunability of work functions through the use of 4-nitrophenylphosphonic acids and 4-cyanophenylphosphonic acids.[26] Both phosphonic acids exhibited increases of 0.60 and 0.77 eV in their work function with dipole moments of 4.04 and 3.59 at the surfaces with these surface modifications. These results demonstrate the effectiveness of the phosphonic acid based monolayers in tuning the surface properties of ITO. However, there is still room for improvements to the results achieved using phosphonic acid based monolayers on ITO.

Table 1.2   **Work functions and surface energies reported for series of phosphonic acid surface modifications on ITO.**

chemical structure	work function (eV)	surface energy (mJ/cm^2)	reference
n-octadecylphosphonic acid	4.5	29	26
phenylphosphonic acid	4.51	N/R*	45
3,3,4,4,5,5,6,6,7,7,8,8,8-tridecafluoro-octlyphosphonic acid	5.1	24	26
pentafluorobenzyl phosphonic acid	4.9	36	26
4-(trifluoromethyl)benzylphosphonic acid	5.4	30	34
tetrafluorobenzyl-1,4-diphosphonic acid	4.5	38	26
TPA-PA	4.58	N/R*	45

 TPD-PA	4.54	N/R*	45
 (trichloromethly)phosphonic acid	5.3	N/R*	47
 4-nitrophenylphosphonic acid	5.6	N/R*	25
 4-cyanophenylphosphonic acid	5.77	N/R*	25

N/R* = not reported in the literature

Phosphonic acids have multiple binding modes with ITO surfaces, which leads to large uncertainties in its stability.[12, 25, 28] The most prevalent mode of binding is bidentate, while the strongest and the most stable binding mode is tridentate on the surfaces of ITO. Having unbound hydroxyl groups hinders the close packing of the molecules within the monolayers and exposes In-O-P bonds making them more susceptible to hydrolytic damage. Studies have shown that phosphonic acid molecules that are bound to ITO surfaces through bi- or mono-dentate modes can undergo hydrolysis and detach from the surfaces while also producing a local increase in acidity.[48] One CV study on ITO modified with phosphonic acids reported that after 60 scans, the faradaic peak increased three-fold, indicating an electrochemical instability.[49] Although phosphonic acid based monolayers offer multiple benefits over silane monolayers and unmodified ITO, due to this low hydrolytic stability, another surface modification was sought for modifying the ITO surfaces. In the research presented within this thesis work, an alternative type of monolayers on

ITO surfaces that utilizes alcohol reagents was pursued and evaluated using several characterization techniques.

1.2. Organic Light Emitting Diodes

One of the most common devices that utilize ITO are OLED displays. In this type of display devices, ITO supported on a glass substrate is used as a transparent anode. The basic schematic diagram of an OLED device is depicted in Figure 1.2. The working principle of OLED displays is that electrons from the cathode and holes from the anode are injected toward the middle light emitting layer in the sandwiched structure.[50] Once electrons and holes join to combine in the light emitting layer, the relaxation of the electrons release energy to the surrounding, exciting organic molecules to emit light. According to this principle, a cathode, an organic light emitting layer, and an anode are required to emit light. Because of the large work function mismatch between those materials, OLED devices were very inefficient as a large amount of energy was required to operate.[1, 50] Over the last few decades, OLED devices underwent many design changes and evolved to contain multiple additional layers that include an electron injection layer, an electron transport layer, a HIL, and a HTL.[1] Through having multiple layers, hole and electron injection processes became step-wise processes, resulting in multiple small energy barriers, instead of one large energy step. By minimizing the sizes of the energy barriers, OLED devices can operate at lower potentials, meaning lower energy consumption and longer lifetimes due to fewer electrochemical stresses.[1, 5, 51-52] This multilayer design yielded brighter and more efficient OLED devices, but there is still room to enhance performance through minimizing those energy barriers and maximizing the physical contact between ITO and the organic layer.
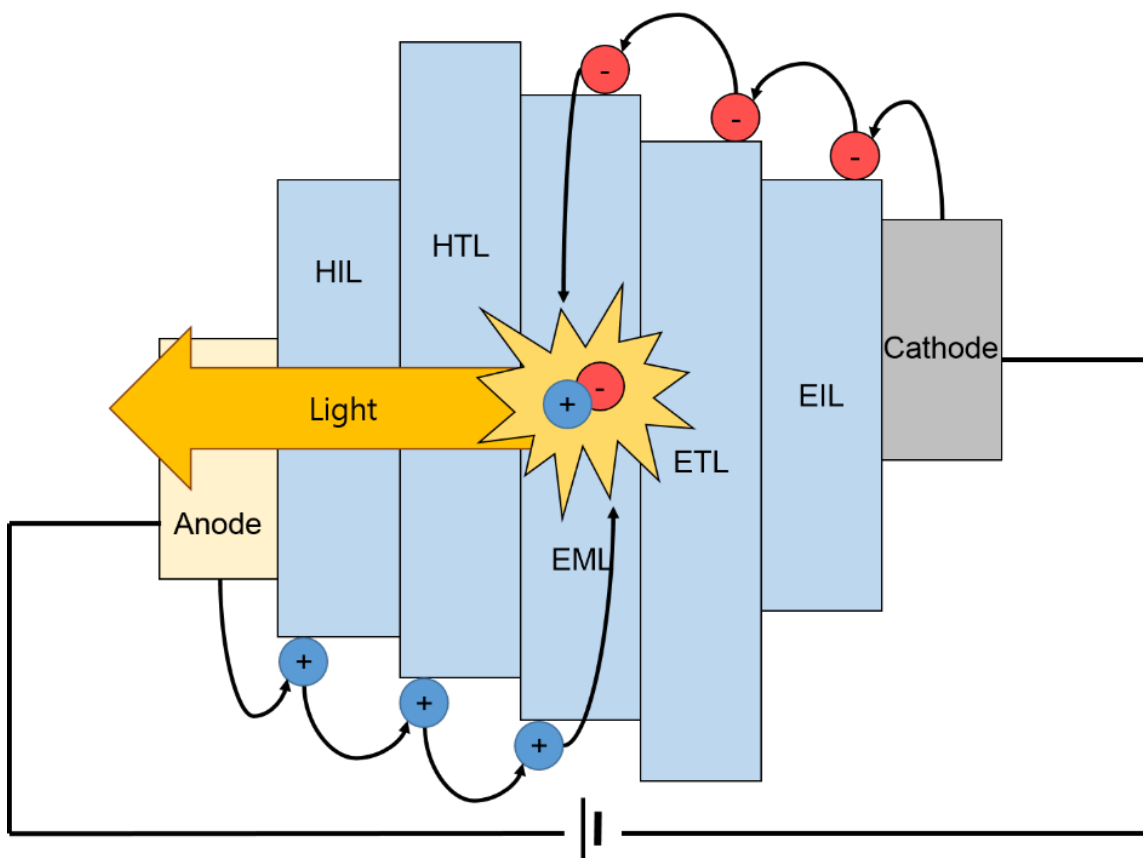
Figure 1.2 **Graphical depiction of OLED working principles. The anode in this figure is ITO and the interface between the ITO and HIL can be modified using monolayers.**

There have been efforts to minimize energy barriers through redesigning the OLED device through insertion of additional layers. These layers can be inorganic and organic materials, such as poly(3,4-ethylenedioxythiphene)polystyrene sulfonate (PEDOT:PSS) that can vary in their thickness from an ångstrom to hundreds of nm.[1] These layers can serve as "support layers". Support layers, often called transport and injection layers, lower each of the transport energy barrier down to smaller energy steps (in some OLED devices, HIL and EIL are absent). These multilayer OLED devices operate more efficiently as less energy is required for the electron or hole transport. Support layers have been studied extensively and the details of these materials and their function are not discussed further in this thesis; further details can be found in the literature.[1, 15, 18, 23] Depending on the materials used to fabricate an OLED device, the size of the energy barriers can vary from 1 to 2 eV. Typically, clean native ITO exhibits a work function of 4.6 eV and phosphorescent molecules deposited on ITO to emit light possess a work function of 5.5

to 6.5 eV.[1] Additional studies have increased the work function of ITO to 6.13 eV through chlorination of these surfaces.[51] The use of UV light to ionize chlorine gas to chlorine ions, which was exchanged with hydroxyl groups at the surfaces of ITO, led to this achievement. This result indicates that hole transport and hole injection layers can be eliminated and still have very energy efficiencies for display devices. Other studies with the use of a series of phosphonic acids have utilized silanes and phosphonic acids to achieve work functions varying from 4.8 to 5.2 eV.[27, 34] Although the work function values achieved through the use of SAMs tend to be lower than that achieved using chlorination of the surfaces, these organic based monolayers offer additional benefits, such as chemical passivation for the ITO for improved chemical and electrochemical stability, tunable surface energies for enhanced electronic contact efficiencies, and a platform for further surface modifications. Because SAMs can be utilized to simultaneously tune multiple properties and provide benefits, they are essential components in OLED devices to optimize their performance.

1.3. Objectives of the Thesis

The main purpose of this thesis work is to investigate an alternative class of monolayers for modifying the surfaces of ITO using alcohol based reagents (Figure 1.3). The alcohol based monolayers aim to achieve high electrochemical, chemical, and optical stabilities of ITO, thereby enhancing the performance and elongating the lifetime of devices that utilize ITO, namely OLED devices. Previous studies have shown a high degree of hydrolytic stability for alcohol based monolayers on other semiconductor surfaces that include silicon and silicon oxide.[53-57] Based on these studies, alcohol based monolayers were grafted on ITO films. The alcohol based monolayers also offer multiple additional benefits including various terminal functional groups and cost effectiveness of reagents relative to silanes and phosphonic acids. The characterization of techniques for evaluating the stability of the alcohol based monolayers on ITO will be discussed in further detail in Chapter 2.
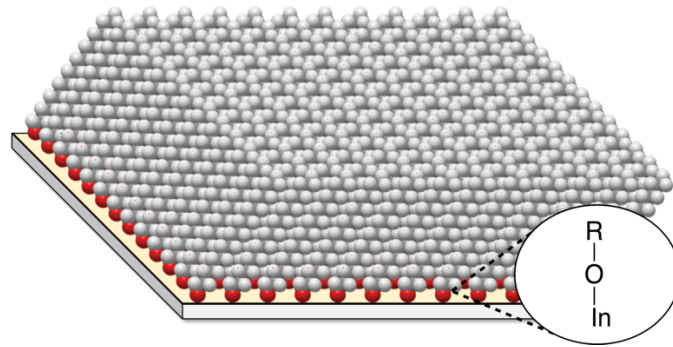
Figure 1.3 **Proposed alcohol based monolayers on ITO.**

Chapter 2.

Characterization Techniques for ITO Surfaces

Monolayers derived from silanes, phosphonic acids and alcohols are characterized using multiple techniques to evaluate their stability, and to study their chemical composition and interfacial properties. The details on these characterization techniques will be discussed in each of the following sections. Critical assessments of these characteristics are required before implementing ITO modified with alcohol based monolayers in organic electronics, such as OPVs and OLEDs.

2.1. Three Electrodes Electrochemical Setup

All TCOs exhibit electrochemical properties that can be varied using different material compositions. The SAMs on TCOs alter these properties by electrochemical insulation of the surfaces, which is often referred as blocking effects.[58] Previous work on SAMs on conductive materials have extensively characterized for these effects.[49, 59-62] To study the blocking effect, a systematic setup is required to assess the electrochemical properties of SAMs on the ITO. In this thesis, to assess the blocking effects, electrochemical properties and performance, alcohol based monolayers were subjected to electrochemical experiments. In these experiments, an electrochemical setup was employed for monitoring processes that occur at the electrode/electrolyte interfaces when an electric potential is applied to electrodes. To accurately monitor these processes, a precise electric potential must be applied to the electrodes and the electric current must also be measured accurately. A three electrodes electrochemical setup enables an accurate measurement of both the electric potential and current. In this thesis, a three electrodes setup consisted of a working electrode (WE), reference electrode (RE) and counter electrode (CE). This setup is utilized to evaluate electrochemical properties of the alcohol based monolayers on ITO electrodes (Figure 2.1).[49, 62-63] Electrochemical analyses were required to study the properties of monolayers on the ITO as it enables assessing multiple surface properties, including the pin hole defects, electron transfer, and the chemical stability provided if the experiment were conducted in a aqueous solution containing high salt concentrations. In this research, all electrodes were partially immersed

in electrolyte containing a conductive solution medium (1 M KCl). In aqueous systems, one of the common materials for RE and CE are Ag/AgCl and Pt rod, respectively.[64] The WE, ITO modified with monolayers prepared in this study, is the electrode being evaluated for its performance in this system. The WEs were cut into 1 cm x 2 cm sections, where only 1 cm x 1 cm was submerged in the 1 M KCl solution to evaluate the properties and performance of the modified electrodes. The RE is an electrode with known constant composition so that known electrochemical processes always occurs at this electrode and that it accurately measures the current flow between RE and WE. The Ag/AgCl RE used in these studies is suitable for the scan rates, either 50 or 200 mV s^{-1}, used in this thesis. The CE is the primary electrode in this setup that measures the applied electric potential. All three electrodes are connected to a potentiostat, which allows the application and control over a potential at the WE, which is needed to determine the electrochemical properties and performance of the WE. In this thesis, temperature control and gas purging were not performed as they were not required to evaluate the monolayers on the ITO.
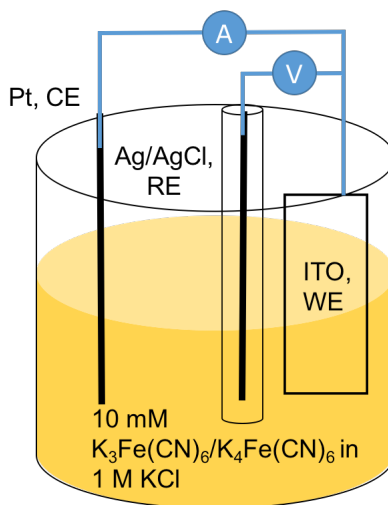
Figure 2.1   A schematic diagram of three electrodes system setup used for CV to evaluate and characterize electrochemical properties of monolayer modified ITO.

2.2. Cyclic Voltammetry Experiments

Cyclic voltammetry (CV) is an electrochemical technique that utilizes a potentiostat and the three electrodes electrochemical setup to study the electrochemical processes occurring at the WE interface with electrolyte.[64] In some cases, redox agents are used to

17

accurately monitor the electrochemical processes. Commonly used redox agents in electrochemical experiments include ferrocene, ferri- and ferro-cyanide and diazonium salts.[65] This technique has a set desired potential range (e.g., 0 to 1 V) that is applied to the WE. The electric potential of the WE is linearly scanned in the forward and backward direction between two low (E_1) and high (E_2) potentials, while measuring current flow. The measured current is the sum of both faradaic and non-faradaic processes. Faradaic processes include oxidation and reduction reactions at the electrodes, and non-faradaic processes represent capacitive current (e.g., double layer charging). In this thesis work, CV is employed to assess the electrochemical and chemical stability of monolayers on ITO surfaces through probing small defective areas (e.g., pin-hole defect) within the monolayers, which is observed through shifts in the faradaic peak position and changes in the faradaic peak current (Figure 2.2). In this thesis, a Pt rod, and Ag/AgCl electrode were employed as the CE and RE, respectively.

The measured current in a CV experiment is mainly dictated by two processes: activation and diffusion controls.[66] Activation control is the kinetic component of the electron transfer process. The electron transfer occurs between the working electrode and the indicators. For example, at the oxidation peak, chemical species at working electrode are being oxidized while indicators in the solution are being reduced. The diffusion control is the mass transport component of the electron transfer process, which can be described by indicators coming sufficiently close to the surface of the working electrode for oxidation/reduction processes to occur and leave this interface. Equation 2.1 captures the relationship between activation and diffusion control, as well as how they contribute to measured current. J_{ac} and J_{diff} represent the activation and diffusion control, respectively.

$$\frac{1}{J} = \frac{1}{J_{ac}} + \frac{1}{J_{diff}} \qquad\qquad Equation\ 2.1$$

In CV, $J = J_{ac}$ initially dictates the current at E_1 as $J_{diff} >> J_{ac}$, but as the magnitude of the applied electric potential increases while scanning to higher potentials, J_{ac} increases while J_{diff} decreases. This process leads to a continuous increase in J until both components are approximately equal. When $J_{ac} = J_{diff}$, J reaches its maximum, the observed faradaic peak current in a CV profile. At this maximum, the surfaces of the working electrode have been fully oxidized and now the process is dictated by the mass transport component rather than the electron transport. In other words, after reaching this maximum J, as applied

electric potential continues to increase, $J_{ac} >> J_{diff}$ and $J = J_{diff}$, and the observed current decreases.
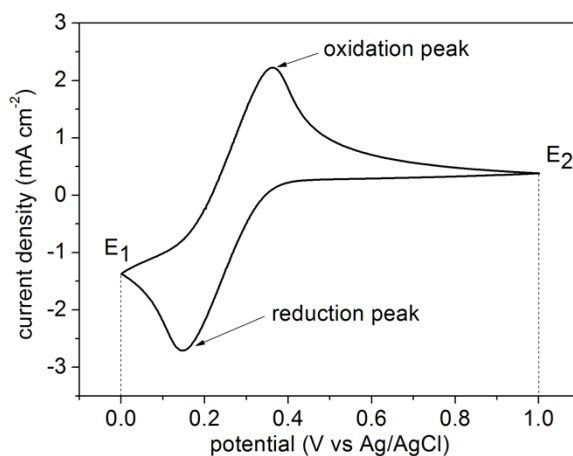
Figure 2.2   **A typical CV scan of native ITO, indicating oxidation and reduction peaks, as well as low and high applied potentials (E_1 and E_2, respectively).**

Oxidation and reduction peak positions are dependent on the RE used in the system, but theoretically for ideal one electron process, the separation distance between the two peaks should be 59 mV.[67-68] This separation distance does, however, depend on the electron transfer kinetics. Decreasing electron transfer rates by an increase in the resistivity (e.g., solution resistivity, and surface resistivity) leads to a larger peak separation distance.[69] The solution resistivity can be ignored in this setup, as 1 M KCl would provide sufficient conductivity. There are two major sources of resistivity with ITO electrodes: surface contaminants, and thickness of the surface oxide layer. The commercial ITOs are often covered with an organic protective layer, which can hinder the electron transfer rates. An appropriate cleaning procedure is, therefore, required to eliminate this organic layer. Changes in the thickness of oxide layer has been observed with different cleaning procedures. As oxygen vacancies in the ITO lattice can contribute to conductivity through providing a free electron, through the use of vigorous cleaning procedures that can oxidize the surfaces these vacancy sites can be filled with oxygen species. This process will reduce the total number of free electrons, which leads to an increase in resistivity and a larger peak separation distance (see further details and discussion in Chapter 3). Peak separations could be caused by the presence of SAMs on the surfaces of the working electrode. Depending on the thicknesses and coverages of

the SAMs, the observed peak currents and peak positions can also vary from those observed for unmodified surfaces.[70]

In this thesis, CV was performed in an aqueous solution, containing redox agents and electrolytes. The scanned potential range was set between 0 to 1 V relative to the CE, using ITO as the WE. This specific range of potentials was chosen to eliminate electrolysis of water at 1.23 V and Fe deposition on ITO at negative potentials.[71] Small redox agents, 10 mM of each $K_3[Fe(CN)_6]$ and $K_4[Fe(CN)_6]$ (oxidation potential at 0.37 V at 25°C)[72], were used to probe pin hole defects within monolayers on ITO surfaces. These redox agents were selected based on their sizes to probe pin hole defects, as these molecules have a smaller in size among other agents that include ferrocene.[58] The concentration (10 mM) was chosen to avoid the depletion of each species. This CV analysis was performed in aqueous 1 M KCl solution to minimize the loss of conductivity and maximize the performance of the electrodes. The applied potential was scanned forward and backward 10,000 times from 0 to 1 V at a rate of 50 mV s^{-1} to observe changes in the faradaic peak position and the peak current density. These observed changes were used to evaluate the stability of each of the monolayers on ITO. Moreover, these observed changes will indicate changes in the interfacial chemistry, such as hydrolysis and degradation of the monolayers prepared monolayers on ITO. As CV is carried out in an aqueous solution containing 1M KCl, it will also simultaneously evaluate the chemical and hydrolytic stability of the monolayers.

2.3. Contact Angle Measurements

Contact angle (CA) measurements are techniques that can be used to quantify the wettability of a liquid (e.g., water or hexadecane) on solid surfaces. It is also one of the most common techniques used to evaluate monolayers on surfaces. This technique requires measuring the angle using the protractor on goniometer. As this technique relies on the manual measurements from an operator, it has shortcomings in consistency, reproducibility, as well as errors for contact angles lower than 20°. A small liquid droplet (2 to 10 μl) is placed on the surfaces of solid, using a micrometer pipette, and the angle between the baseline (solid-liquid interface) and tangent line to the liquid droplet at the bottom (liquid-gas interface) is measured to obtain the CA (Figure 2.3). It represents where

three interfacial tensions γ_{SG}, γ_{SL} and γ_{LG} are at the equilibrium. The values of these interfacial tensions vary with the species of the liquid, the surfaces of the solids and the atmosphere of where the measurements are taken. This equilibrium can be described by the Young's equation (Equation 2.2), where θ_c represents the measured CA.[59, 73] γ_{SG}, γ_{SL} and γ_{LG} represents for solid-gas, solid-liquid and liquid-gas interfacial tensions, respectively.

$$\gamma_{SV} - \gamma_{SL} = \gamma_{LV} \cos \theta_c \qquad \qquad Equation\ 2.2$$

Typically, if the measured CA with a water droplet is below 90° (Figure 2.3A), the solid surface is considered to be hydrophilic, or in a high wetting state, as:

$$\gamma_{LV} \cos \theta_c > 0$$

$$\gamma_{SV} - \gamma_{SL} > 0$$

$$\gamma_{SV} > \gamma_{SL}$$

As the interfacial tension between solid-gas is larger than at the solid-liquid interface, the solid-gas tension pulls the droplet outward, decreasing the CA. If the measured CA is between 90° and 180° (Figure 2.3C), the solid surface is considered hydrophobic, or in a low wetting state, as $\gamma_{SV} < \gamma_{SL}$.
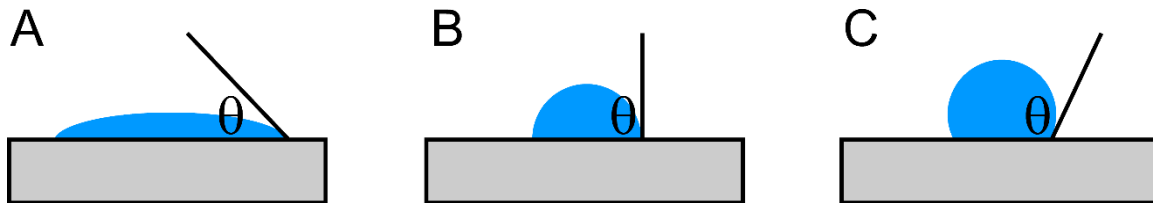
Figure 2.3 **Contact Angle (CA) Scenarios. The obtained CA can determine the wetting of the surface: A) high wettability; θ < 90°, B) boundary condition, θ = 90°; and C) low wettability, θ > 90°.**

There are different approaches to study the surface energies of solids, which include the work of adhesion (Equation 2.3), the Young-Dupré equation (Equation 2.4), the Young-Fowkes equation (Equation 2.5) and the Owens-Wendt model (Equation 2.6).[59, 73-74]

$$W_{12}^a = \gamma_1 + \gamma_2 - \gamma_{12} \qquad\qquad Equation\ 2.3$$

$$W_{SL}^a = \gamma_{SV} + \gamma_{LV} - \gamma_{SL} \qquad\qquad Equation\ 2.4$$

From the Young-Dupré equation, Fowkes made a first approach to partition the surface energy into its disparate components.[59, 73] It was proposed that the measured surface energy is a sum of multiple components that include the dispersive, polar, hydrogen bonding, induction, and acid-base contributions. His approach involved investigating dispersive interactions between the solid and the liquid as follows:

$$W_{SL} = \gamma_S + \gamma_L - 2\left(\gamma_S^d \gamma_L^d\right)^{0.5} \qquad\qquad Equation\ 2.5$$

From the Young-Fowkes equation (Equation 2.5), Owen and Wendt pursued further partitioning the surface energy. They proposed that dispersive and polar components (γ_i^d and γ_i^p) are dominant terms in surface energy (Equation 2.6). Similar to what Fowkes had proposed, they also took the geometric mean of surface tensions. Their revised expression is derived as follows:

$$W_a = 2\left(\sqrt{\gamma_{SV}^d \gamma_{LV}^d} + \sqrt{\gamma_{SV}^p \gamma_{LV}^p}\right)$$

$$based\ on\ assumption, \quad \gamma_i = \gamma_i^d + \gamma_i^p$$

$$through\ combining\ with\ Young\ equation,$$

$$\gamma_{SL} = \gamma_{SV} + \gamma_{LV} - 2\left(\sqrt{\gamma_{SV}^d \gamma_{LV}^d} + \sqrt{\gamma_{SV}^p \gamma_{LV}^p}\right),$$

$$resulting\ in\ the\ derivation\ of\ the\ Owens - Wendt\ equation:$$

$$\gamma_{LV}(1 + \cos\theta_c) = 2\left(\sqrt{\gamma_{SV}^d \gamma_{LV}^d} + \sqrt{\gamma_{SV}^p \gamma_{LV}^p}\right) \qquad Equation\ 2.6$$

The Owens-Wendt equation offers a route to calculating the dispersive and polar interactions at the solid-liquid interfaces. In order to determine each component, liquids

that are very polar, such as water, or that are very non-polar, such as hexadecane, are typically used to measure the contact angles. In this thesis, as surface polarity is directly related to the surface energy and work function, the Owens-Wendt model was used to measure each component.

2.4. X-ray Photoelectron Spectroscopy

X-ray photoelectron spectroscopy (XPS) is a surface analysis technique that provides information about chemical compositions. The working mechanism of the XPS is through irradiating the sample and its surfaces with monochromatic X-rays. The XPS is a surface-sensitive technique because of the penetration of the resulting photoelectrons. The penetration depth of these photoelectrons depends on the inelastic mean free path (IMFP) of an electron, which varies with the energy of the generated X-rays and composition of material under study.[75] The common sources of these X-rays include Al and Mg.[75-76] In this thesis, X-rays generated from aluminum source (1487 eV) were utilized to investigate the chemical composition of samples. The resulting photoelectrons for the modified ITO surfaces have a penetration depth of approximately 10 nm. Samples are irradiated with the generated X-rays, which causes the sample to eject an inner shell electron (a photoelectron). The kinetic energy of the ejected photoelectron is detected by an electron energy analyzer. The principles of XPS are based on the photoionization and the Koopman's theorem, assuming there will be no relaxation of the excited electron following the photoemission.[75-76]

$$E = hv, \; energy \; of \; a \; photon \qquad\qquad Equation \; 2.7$$

$$A + hv \rightarrow A^+ + e^-, photoionization \qquad Equation \; 2.8$$

$$E(A) + hv = E(A^+) + E(e^-) \qquad\qquad Equation \; 2.9$$

$$as \; E(e^-) = E_K \; and \; through \; rearranging,$$

$$E_K = hv - (E(A^+) - E(A)) \qquad\qquad Equation \; 2.10$$

$$E_B = E(A^+) - E(A), Koopman's \; theorem \;\; Equation \; 2.11$$

23

$$E_K = hv - E_B \qquad\qquad\qquad Equation\ 2.12$$

Combining the energy of a photon (Equation 2.7, where h = plank's constant and v = frequency) and photoionization (Equation 2.8) and considering the conservation of energy, a new term is derived for photoionization (Equation 2.9). As energy of an electron in this case is equal to kinetic energy (E_K), Equation 2.9 can be re-written as Equation 2.10. The Koopman's theorem, which describes a binding energy of an electron (Equation 2.11) and when it is combined with Equation 2.10, a new equation is derived for an overall photoionization (Equation 2.12). Although this equation accurately reflects the process occurring at the sample, it requires a correction factor, accounting for the effects of the analyzer. For the instrumentation used to measure the binding energies, the changes are typically measured with respect to the Fermi-level (E_F) instead of the vacuum level (E_{vac}). Therefore, the work function of the spectrometer must be accounted for in order to produce an accurate measurement as shown:

$$E_K = hv - E_B - \Phi \qquad\qquad Equation\ 2.13$$

$$rearranging,\ E_B = hv - E_k - \Phi \qquad Equation\ 2.14$$

Through the use of Equation 2.14, the binding energy of the ejected photoelectron can be calculated based on the kinetic energy of the photoelectron detected by the analyzer. Each binding energy is unique to the element and the orbital of the electrons interacting with the incident X-rays, which enables the study of the chemical bonds that are present between atoms and their oxidation states in the surfaces of the materials. A survey plot of E_B versus the count rate has a large background noise due to inelastic collisions of emitted electrons within the sample. This background noise can be seen in the spectrum as indicated in Figure 2.4.

Another important aspect in XPS analysis is the orbital information found in a spectrum. As shown in Figure 2.4, each peak in binding energy is assigned to a specific orbital of an element. All orbital levels, except s orbitals, exhibit doublet splitting patterns due to spin-orbit splitting.[75-78] According to crystal field splitting of d orbital energy levels, d orbitals exhibit doublet splitting patterns in the ratio of 2:3, when quantifying the surface chemical composition through integration of XPS peaks. The 3d orbitals exhibit a

degeneracy in their orbital structure.[76] The 3d orbitals have a principle quantum number (*n*) of 3, an angular momentum quantum number (*l*) of 2 and the spin angular momentum quantum number (*s*) of $\pm 1/2$. These quantum numbers give rises to 2 different energy levels, which are the $3d_{3/2}$ and $3d_{5/2}$ states. Because some peak positions differ by less than 1 eV, convoluted peaks often appear with the acquired spectrum. The 3d orbitals from In and Sn exhibit the same splitting patterns. Each of these peaks present in the spectrum can be deconvoluted and assigned to a correct orbital of an element based on the binding energies and the quantum numbers. Although survey XPS scan can provide chemical species present in the sample, it does not provide information on the ratio of the composition. To quantify such information, high resolution spectra of those XPS peaks are required to analyze and deconvolute the data.

High resolution XPS spectra provide information on a specific element and the orbital from which the photoelectrons were ejected. Elements in different oxidation states and/or coordinating with different species can give rise to difference in peak positions. High resolution spectra enable a determination of surface chemical compositions.[75-76] Through quantification and peak fitting, individual components of a peak can be resolved, which enables an analysis of the relative compositions within the sample. For example, SAMs on metal oxide surfaces often require analyses of oxygen 1s high resolution spectra to acquire information on the species present and their bonding environment. The resulting high resolution spectrum will have a convoluted peak that contains all of the oxygen species present at the surfaces. Deconvolution of the peak through a fitting routine gives the relative contributions from different oxygen species can be identified and quantified. In this thesis, the surfaces of ITO were studied through oxygen high resolution spectra. All surface modifications on ITO, such as silanes, phosphonic acids and alcohols, utilize the oxo and/or hydroxyl groups at the surfaces. Therefore, oxygen high resolution spectra enable a determination of the surface compositions.
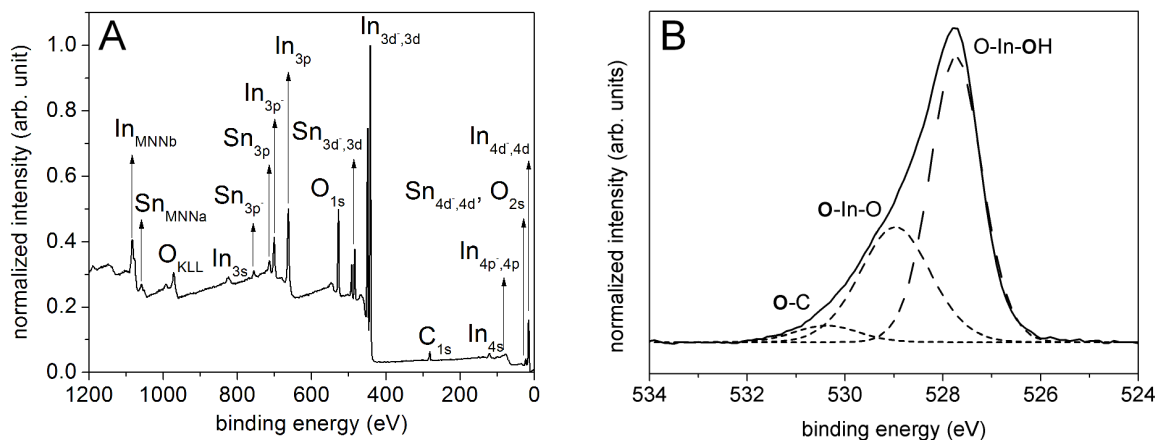
Figure 2.4   A typical survey XPS scan (A) and a typical oxygen high resolution XPS scan (B) of an ITO coated substrate.

2.5. Ultraviolet Photoelectron Spectroscopy

Ultraviolet photoelectron spectroscopy (UPS) is a technique to study band structures of materials and is commonly used to assess the electronic properties of materials widely used in the semiconductor field.[75, 79] The working principles of UPS are the same as XPS, which involve the photoionization of electrons and are based on the Koopman's theorem.[79-80] The primary difference between the two techniques are in the radiation source. In UPS, ultraviolet light generated from noble gases (e.g., He 1 & 2 and Ar) is used as the prepared radiation source, instead of X-rays (Figure 2.5). Using UV photons as an radiation source allows probing the band structure of the sample as the photon energy is much lower than the X-ray energy (21.2 eV for He 1 source, compared to 1487 eV for aluminum source).[79-80] Because of the low energy radiation, the penetration depth of UPS is approximately 2 nm. Although using low energy photons to study surfaces enables acquisition of information on band structures, along with an extreme surface sensitivity, it complicates the design of the instrumentation (Figure 2.5). Since photons interact with all known materials, the radiation source to the analysis chamber is not a closed system. This analytical technique requires an ultra-high vacuum environment. To minimize contamination and achieve the ultra-high vacuum status, two pumps are attached to an outlet that is connected to the chamber. Because of this possible contamination, noble gases are the common radiation sources used to generate photons. These noble gases are also inert, which enables acquisition of data without damaging the sample. The presence of noble gases inside the analysis chamber and the requirement

26

for it be an open system means that UPS operates at a lower vacuum than XPS. The UPS also requires applying a small potential electric potential (e.g., from a 5 V battery) to eliminate background noise from noble gases.
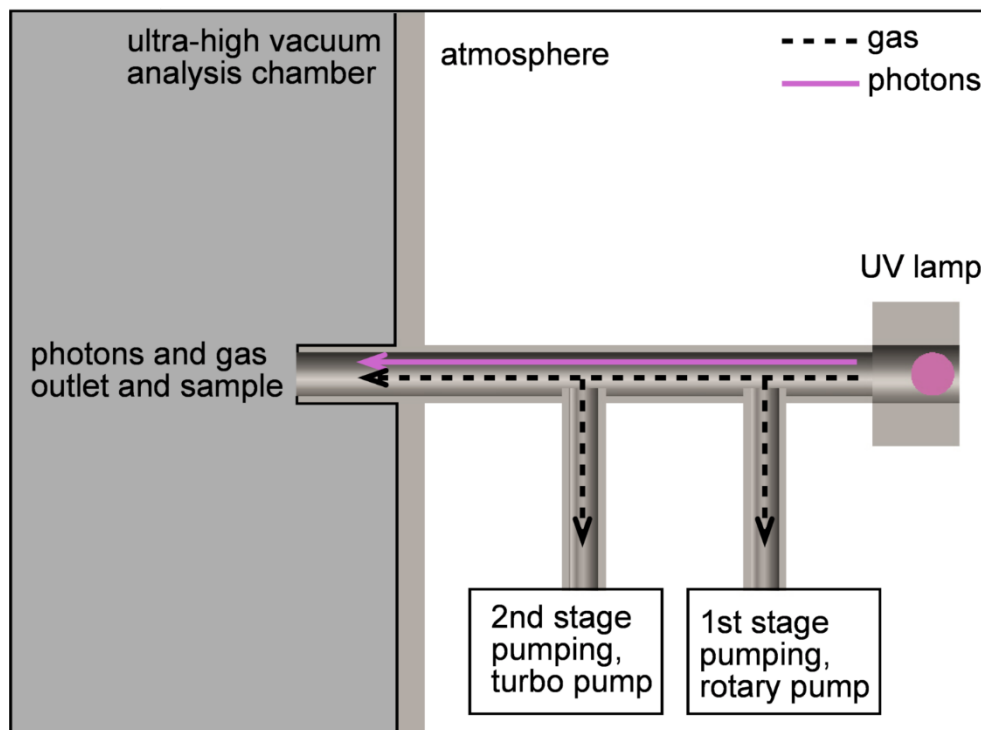
Figure 2.5   A schematic illustration of UPS instrumentation.

While XPS can eject the core shell photoelectrons, the low energy photons used in UPS do not have the sufficient energy to eject the inner photoelectron. They eject electrons from the valence band instead. The band structure can, therefore, be investigated using this technique. The UPS can yeild information on work function, Fermi levels, and valence band maxima for inorganic materials (Figure 2.6).[75, 79] For organic materials, the highest occupied molecular orbital (HOMO) and lowest unoccupied molecular orbital (LUMO) can be obtained from the acquired UPS spectra.[79-80] For the scope of this thesis, only the work function will be determined from UPS spectra and discussed in detail.
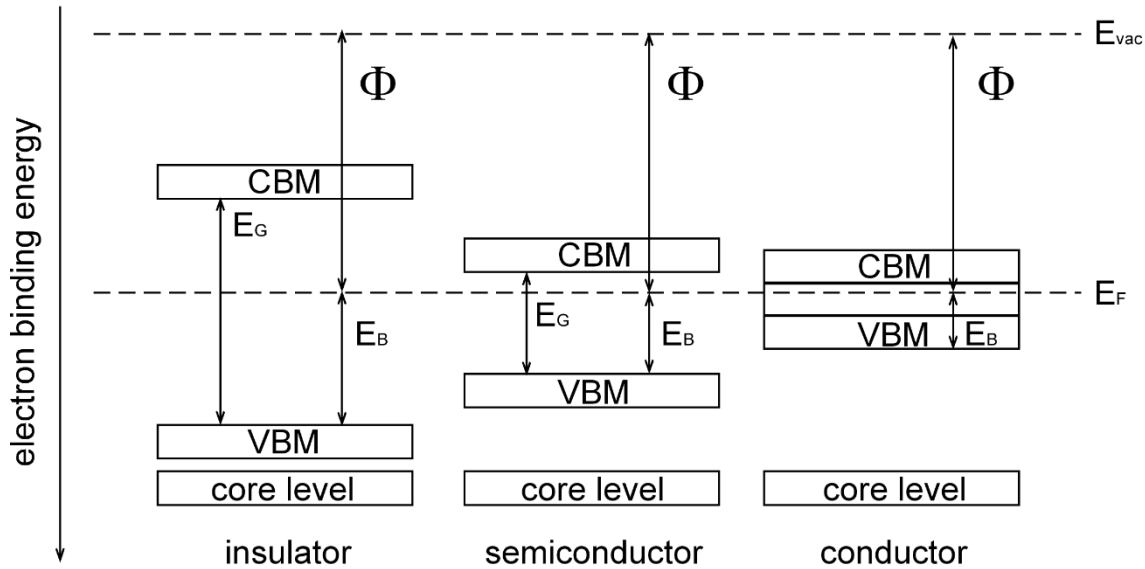
Figure 2.6 **Energy diagram representing work function (Φ), band gap (E_G) and binding energy (E_B) in an insulator, a semiconductor and a conductor.**

The work function refers to the energy required to pull a single electron from the Fermi level to the vacuum level.[81] There are multiple methods to measure work functions, including UPS and Kelvin probe.[1] Measuring the work function using Kelvin probe techniques will not be discussed here. In contrast to XPS, UPS is a qualitative technique because detected electrons by the spectrometer have gone through inelastic collisions. The shape of UPS spectra depends on the sample material (e.g., conductor, semiconductor, or insulator).[79] For all clean surfaces, such as Au, the E_F is always at 0 eV on the UPS spectrum, where the Fermi-edge is observed, while modified surfaces may exhibit shifts in the E_F. For conductors, which have overlapping conduction bands (E_{CBM}), and valence bands (E_{VBM}), and the Fermi level within those bands, there are two important edges of the spectrum: the Fermi-edge and secondary electron cut-off edge (E_{SEC}), which defines the width of the spectrum. This width subtracted from the maximum kinetic energy of the source determines the work function. For insulators and semiconductors, such as ITO, because of the presence of the band gap, the Fermi-edge does not appear. The E_F is still at 0 eV and instead of the Fermi-edge, E_{VBM} appears within the spectrum (Figure 2.7). Therefore, the width of the spectrum is still used to calculate the work function of the sample material.
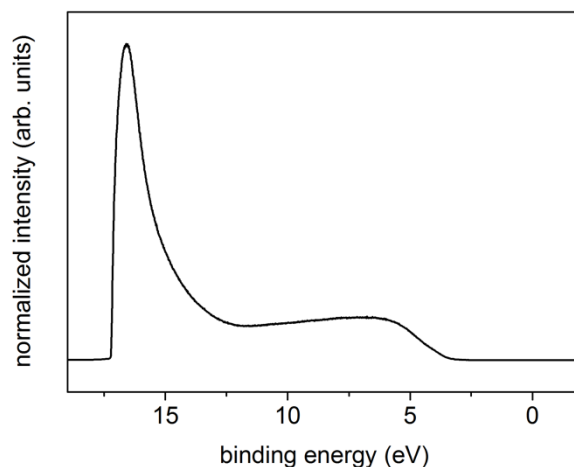
Figure 2.7   A typical UPS spectrum of clean native ITO

In the case of modified surfaces, there is one additional component that needs to be taken into account, E_{VBM}. Modified surfaces can cause shifts in energy levels through two mechanisms, band bending and surface polarity. Band bending and dipole moments induced by the modification of ITO with monolayers can shift the positions of the E_F and E_{VAC}.[81-82] According to the Schottky-Mott rule and Fermi-level pinning, band bending occurs when two different materials come into contact.[83] Their energy levels re-align using E_F as their reference. All energy levels, except E_F, including the E_{VAC}, E_{VBM}, E_{CBM}, HOMO and LUMO will bend accordingly. This process often decreases the work function of ITO in OLED devices because the organic layers have a higher work function, which means that the relative position of E_F for the organic layer is lower than the one for ITO. The ITO-modified with monolayers, through inducing permanent dipole at these surfaces, can increase their work function. This process is dictated by the direction of the dipole moment because it can shift the position of the E_{VAC}.[83] There are two components in determining the position of E_{VAC}: the intrinsic bulk property and the surface dipole.[81] Although the major determinant is the intrinsic bulk property, the surface dipole can be modified to shift the position of E_{VAC}.[81] Electron affinity, which is the energy gained or required to move an electron at the vacuum level to conduction band minimum, is altered by inducing a dipole at the surfaces. If an inward oriented dipole moment is induced, the work function would decrease as the positive charges at the surfaces will decrease the electron affinity, shifting the E_{vac} downward. When outward oriented dipole moment is induced, work function will increase as surface negative charges increase the electron affinity, shifting E_{vac} upward (Figure 2.8). Consequently, measuring the work function of the modified surfaces require

29

determining shifts in the energy levels. These shifts can be seen in the overall shift of the E_{VBM} and can be quantified using the changes in the position of E_{VBM} relative to E_F on the UPS spectra (Figure 2.9). The work function of modified surfaces can be accurately determined using Equation 2.15.[83] Here the work function is represented by Φ, the surface potential by χ, the degree of band bending by eB, the conduction band minimum by E_C, and and the Fermi-level by E_F. The work function of ITO modified with monolayers determines the hole injection barrier when incorporated in organic electronic devices. Minimizing the hole injection barrier is crucial for the improvement of the efficiencies and performances of these devices. Therefore, an accurate determination of the work function of ITO modified with monolayers is critical in evaluating their electronic properties, as well as for future use in devices and electronic applications.

$$\Phi = \chi + eB + (E_C - E_F) \qquad\qquad Equation\ 2.15$$
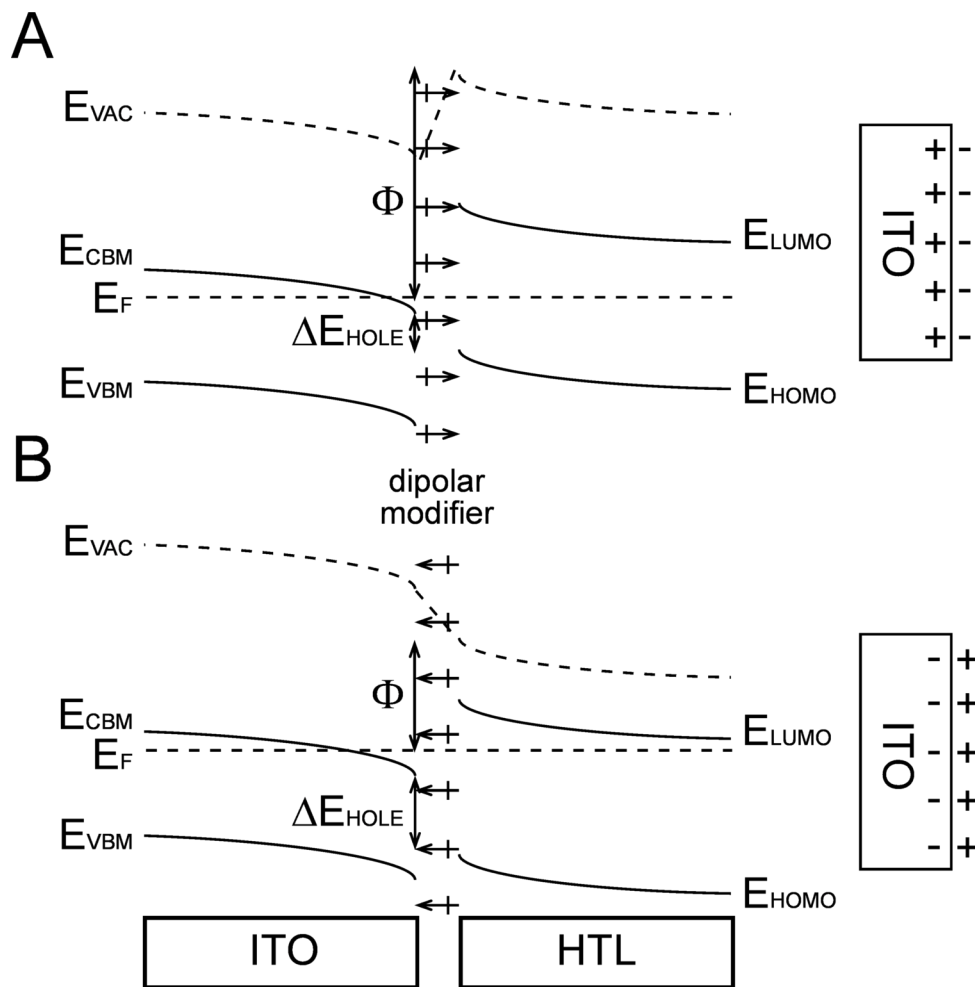
Figure 2.8 **Work function (Φ) and hole injection barrier (ΔE_{HOLE}) tuned through the use of a dipolar modifier at the interface between ITO and HTL. (A) Representation of an outward oriented dipole at the interface between ITO and HTL, while (B) Representation of an inward oriented dipole at the same interface. Only an outward oriented dipole increases the vacuum level to increase work function and minimize the hole injection barrier.**
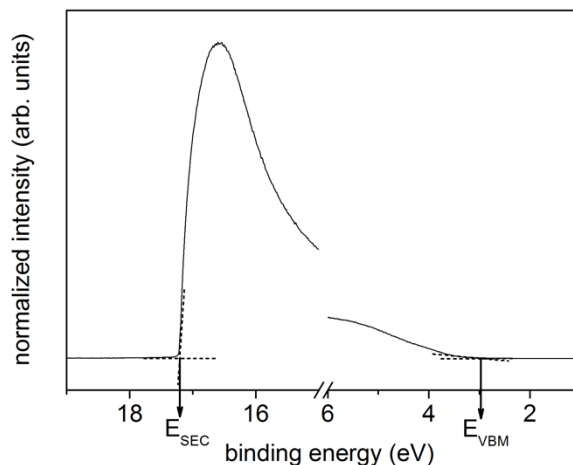
Figure 2.9   A typical UPS spectrum of ITO indicating the secondary electron cut-off edge (E_{SEC}) and valence band maximum (E_{VBM}).

All of the mentioned techniques described in this section were used to characterize the properties of monolayers on ITO. The CV analyses, which utilized a three electrodes system, were employed to assess electrochemical and chemical stability of the monolayers on ITO. The CA measurements enabled an assessment of the changes in surface coverage of the monolayers, as well as to their modified surface energies. The XPS analyses were performed to study chemical compositions of the monolayers on ITO both before and after the series of electrochemical tests. Work functions of the modified surfaces of ITO were measured using UPS techniques, which enabled an evaluation the electronic properties of the alcohol based monolayers on ITO.

Chapter 3.

Alcohol Based Monolayers on ITO surfaces

3.1. Notice of Permissions

A manuscript based on the work presented in this chapter is currently being prepared for publication. The majority of the work presented in this paper has been performed by myself, including experiments, data acquisition and writing, under the guidance of Dr. Byron Gates. Mr. Austin Lee performed the XPS analyses and Dr. Jennie Eastcott provided advice on the electrochemistry section of this work.

3.2. Introduction

Surface modifications of transparent conductive oxides, including indium tin oxide (ITO), have been extensively studied to tune their interfacial properties, such as surface energy and work function.[5, 25-27, 29-31, 47] This modification is necessary to achieve the optimal performance in organic electronic devices and to prolong their lifetime. Often, the interface between unmodified ITO and the hole transport layer (HTL) can undergo multiple degradations, thereby shortening the device lifetime.[1] The hydrophobic non-polar organic HTLs are deposited on ITO in many devices that include OLEDs and OPVs.[1, 5, 27, 31, 47] There is an electronic mismatch between these HTLs and ITO as the two materials often exhibit a significantly higher work function (approximately 1.2 to 1.8 eV).[51] This mismatch, called the hole injection barrier, is directly associated with the efficiency of devices incorporating HTLs and ITO. Work functions of clean native ITO, depending on the procedures used to clean their surfaces, can vary from 4.2 to 5.1 eV.[27, 29-30, 51, 84-85] Another form of mismatch at this interface is the surface energy. This mismach leads to a non-uniform wetting of the organic films and subsequent changes to the interface can lead to delamination of the HTL. Therefore simultaneously tuning both the surface energy and work function of ITO is desired to optimize the performances of organic based electronics. Previously, in an effort to enhance the performance of organic based electronics, the surfaces of ITO have been modified using both inorganic and organic chemistries to adjust the properties of interfaces. Silane and phosphonic acid based derivatives have been

widely used to tune the surface properties of ITO.[3, 5, 25-30, 32-33, 35, 46, 86] Although these strategies can increase the work function and tune the surface energy of ITO electrodes, studies have shown that these modifications can compromise the electronic and/or optical properties of the ITO films after prolonged exposure to operational or environmental stresses.[1, 41, 87] These changes can significantly reduce the performance and operational lifetime of the ITO and, in turn, the electronic devices utilizing its properties.[32, 88-91] Both silanes and phosphonic acid based monolayers do, however, contain potential impurities that can impair device performance. Silane based monolayers may degrade into a thin layer of silicon oxide over time.[92] Monolayers of phosphonic acid are prone to hydrolytic damage because of the varying binding mechanisms of these molecules on ITO (e.g., a mixture of mono-, bi- and tri-dentate).[12, 91]

Here, we report a new heteroatom-free covalent surface modification of ITO using alcohol based monolayers to simultaneously control the resulting surface energy and work function. Similar to other surface modifications using SAMs, alcohols can covalently bond with hydroxyl containing oxide surfaces via the formation of ether bonds (e.g., In-O-R or Sn-O-R). This process is analogous to the surface modifications achieved using silane and phosphonic acid based monolayers (In-O-Si and In-O-P).[5, 25-30, 32-33, 49] We sought to understand the effectiveness of tuning the surface properties of ITO through the use of alcohol based monolayers. These surface modifications were directly compared with ITO electrodes modified with silanes or phosphonic acids. The alcohol based monolayers were characterized using multiple techniques that include prolonged cyclic voltammetry (CV) scans, contact angle (CA) measurements, X-ray photoelectron spectroscopy (XPS), and ultraviolet-visible transmission spectroscopy (UV-Vis). These techniques enabled an assessment of the electrochemical, optical, and chemical stability of the modified ITO films. We also sought to understand the impact of changing the length of the alkyl chains on the alcohol reagents with regards to their passivation of the ITO interfaces. Work functions and surface energies of these alcohol modified ITO films were determined using ultraviolet photoelectron spectroscopy (UPS) and CA measurements to better understand the electronic properties of the modified ITO. These analyses confirmed that the desired interfacial properties were achieved through the use of alcohol based monolayers to attain the desired interfacial properties, and alcohol based monolayers could potentially improve the lifetime of electronic devices that utilize ITO.

3.3. Results and Discussion

Electronic devices that utilize organic electronic materials often incorporate ITO or other transparent conductive oxides (TCOs) at an interface within the device. This interface between these dissimilar materials requires further surface modifications to improve their performance and durability.[34, 48] Numerous different surface modifications have been pursued, but many of these modifications have demonstrated drawbacks that include hydrolytic damage and/or lack of uniformity across this interface.[12, 16, 34] In this study, we prepared a series of monolayers derived from alcohol reagents that include 1-octadecanol (ODA), 1*H*,1*H*,2*H*,2*H*-perfluoro-1-octanol (PFOA), 1,5-pentanediol (PTdiA) and 1,10-decanediol (DCdiA) to demonstrate a new type of SAM on ITO. These modifications to the surfaces of the ITO films are, in many ways, analogous to the preparation of monolayers on silicon oxides. Previous methods to prepare monolayers on silicon oxides from alcohol based reagents include the use of convective or microwave heating, UV-irradiation, or the use of catalysts.[53-57, 93-96] The study described herein extends the application of these reactants to form alcohol based monolayers on ITO and, by extension, to demonstrate their utility for modifying the properties of ITO. Among the alcohol based monolayers prepared in this study, the monolayers derived from ODA were specifically evaluated in a detailed comparison to monolayers that were prepared from octadecyltrichlorosilane (ODTS) and octadecylphosphonic acid (ODPA). All precursor species to these three monolayers consisted of a linear 18 hydrocarbon chain, which was previously demonstrated to form crystalline monolayers due to van der Waals interactions.[27, 29, 53] Prior to any surface modifications, the ITO surfaces were cleaned and oxidized using a modified RCA-1 standard cleaning procedure. Each type of monolayer was grafted onto ITO using specific procedures, which are discussed in detail in the experimental section. Monolayers derived from ODA required heating up to 120 °C in neat solutions of alcohol reagents for 24 h, while ODTS and ODPA monolayers were grafted at room temperature in hexane and tetrahydrofuran (THF) solutions, respectively. These monolayers were successfully prepared from solutions of either 95% or 99% ODA. The contact angles obtained from alcohol based monolayers on ITO that were prepared at lower temperatures (<120 °C) or with the use of solvents, such as propylene carbonate, indicated either the absence of SAMs or a relatively poor surface coverage. Following the formation of the monolayers, each sample was sonicated in ethanol and dried with a stream of filtered nitrogen gas. The RCA-1 cleaned ITO substrates (as a control) and

substrates coated with the monolayers were subjected to multiple characterization techniques to cross-evaluate the stability of the monolayers, as well as to assess their optical and electronic properties.

3.3.1. Electrochemical and Chemical Stability of Alcohol Based Monolayers on ITO

Surface modifications to ITO are required to tune their properties, as well as to minimize their potential degradation by thermal, photochemical and diffusive based processes. A common methodology to design the interfacial chemistry of ITO is through the use of SAMs.[1] To understand the impact and advantages of alcohol based monolayers, their electrochemical and chemical properties were compared to those of silane and phosphonic acid based monolayers. A series of CV, WCAs and XPS measurements were performed to assess the ability of the alcohol based monolayers to tune the properties of the ITO.

All of the monolayers prepared on ITO were subjected to an extensive set of CV experiments. Figure 3.1 depicts 1st CV profiles obtained from different cleaning procedures. Largest peak separation was observed with the RCA-1 cleaned substrate. This separation can be attributed to the reduction in oxygen vacancies, which generates a free electron that contributes to conductivity. In particular, ODA, ODTS and ODPA were used to cross-evaluate their electrochemical stability through these CV experiments. The modified ITO films served as a working electrode submerged in a 1 M KCl solution containing 10 mM $K_4[Fe(CN)_6]$ and 10 mM $K_3[Fe(CN)_6]$. These studies mimicked the use of modified ITO substrates while being subjected to corrosive electrolytic conditioning, which may be experienced by the electrodes after a prolonged use in some electronic devices. Changes in the composition and structure of the monolayers were monitored through the use of small redox reporters (i.e., $K_4[Fe(CN)_6]$ and $K_3[Fe(CN)_6]$) incorporated into the electrolytic conditioning solutions. Changes in the electrochemical peak current density and peak potential of the oxidation and reduction processes were assessed as an indication of changes to the SAMs at the ITO interface. The electric potential applied to the ITO electrodes was continuously scanned between 0 and 1 V versus a Ag/AgCl reference electrode for at least 10,000 full scans or approximately 2.5 days. This range of potentials was selected to avoid the deposition of iron oxide on the ITO at negative

potentials, and the electrolysis of water at 1.23 V.[71] Such parameters enabled an assessment of the electrochemical and hydrolytic stability of each type of monolayers on the ITO substrates.

Although there are many reports on the electrochemical properties of silane or phosphonic acid based monolayers on ITO, to the best of our knowledge, the hydrolytic and electrochemical stability of these monolayers have not been extensively studied. Examples of SAMs on ITO that have been otherwise extensively studied in the literature include those prepared from ODTS and ODPA.[25, 27, 29, 49, 62] In the current study, ITO surfaces modified with ODA were directly compared to ITO surfaces coated with either ODTS or ODPA. Additional control experiments included a comparison to the properties of RCA-1 cleaned ITO. The modification of the ITO surfaces with organic molecules can decrease the current passed through these electrodes, and could also shift the potentials of the oxidation and reduction processes that take place at these electrodes.[97-98] Changes to the monolayers on the ITO, such as a restructuring of the assembled coatings or any decrease in the integrity of these coatings, can further alter the electronic properties of ITO electrodes. The peak current could increase or the peak potential could decrease for the oxidation process due to a loss of the surface passivation. A previous study on the electrochemical properties of monolayers derived from n-alkylphosphonic acid were analyzed by CV techniques.[62] Their results demonstrated a three-fold increase in the oxidation peak current within only 60 consecutive CV scans of the applied potential. Similar results were observed in our CV experiments with ODPA monolayers, where the oxidation peak current almost doubled within the first 100 CV scans. Although hydrolytic instability of ODPA and ODTS monolayers are well understood, this hydrolytic and electrochemical instability has not been studied extensively for their durability on ITO electrodes. In this study, we prepared ODA, ODTS and ODPA monolayers on ITO and evaluated their electrochemical properties and stabilities after extensive CV analysis.
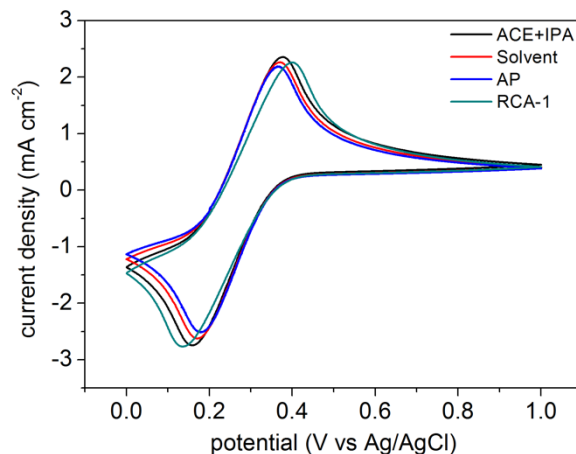
Figure 3.1   **Cyclic voltammetry obtained from native ITO surfaces after applying different surface treatments. Notations are defined as the following: ACE + IPA = sonication in acetone and isopropanol for 10 min each; Solvent = 20 min sonication in Sparkleen® 1 solution and 10 min in acetone, isopropanol and then ethanol; AP = solvent cleaning as described above followed by 5 min of air plasma; and RCA-1 = solvent cleaning as described above followed by 3 h of RCA-1 cleaning procedure.**
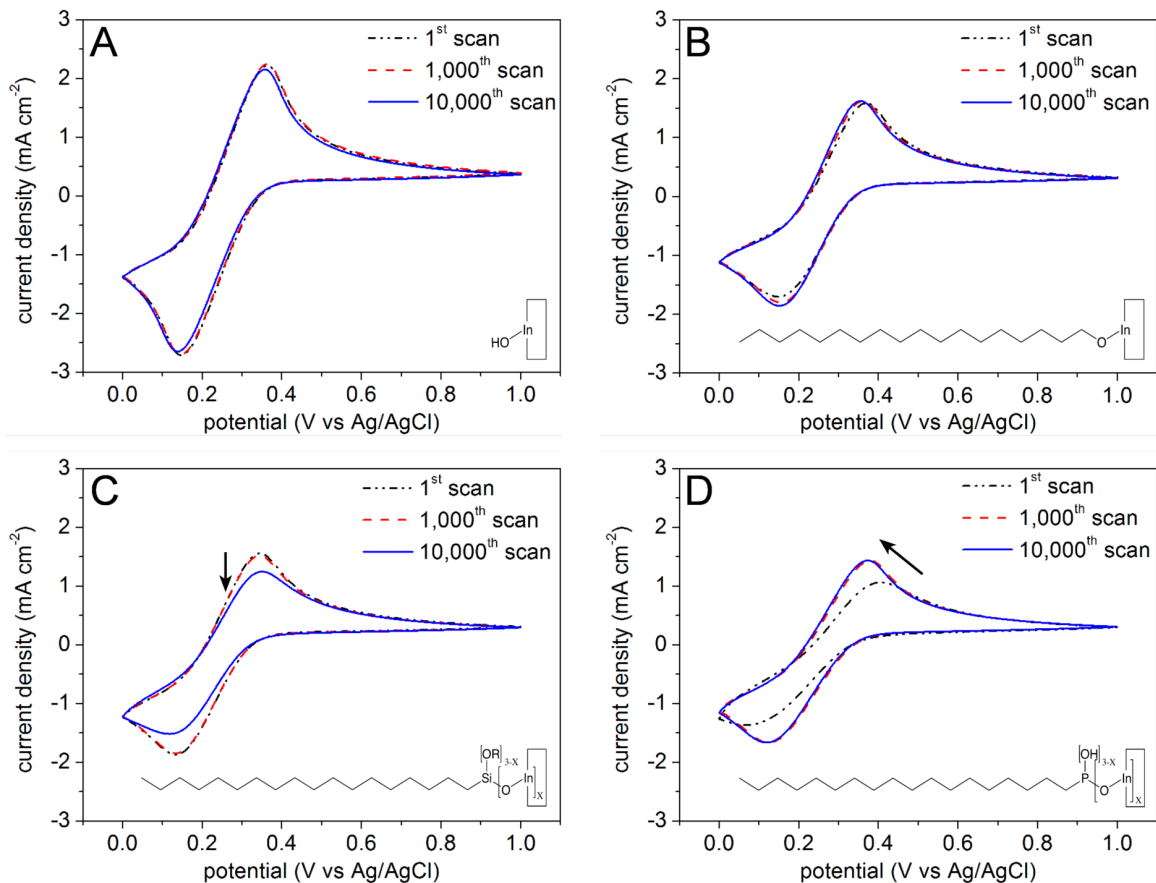
Figure 3.2 The 1st, 1,000th and 10,000th scans of the cyclic voltammetry analyses of (A) RCA-1 cleaned ITO, (B) 1-octadecanol (ODA) coated ITO, (C) octadecyltrichlorosilane (ODTS) coated ITO, and (D) octadecylphosphonic acid (ODPA) coated ITO. These electrochemical studies were performed at a scan rate of 50 mV s^{-1} using the ITO substrates as the working electrode in 1 M KCl solutions containing 10 mM potassium ferricyanide and 10 mM potassium ferrocyanide. Black arrows indicate trends observed in the change in position and peak current of the oxidation processes over the course of these experiments.

We assessed the electrochemical properties of monolayers on ITO electrodes by monitoring for changes in their oxidation peak position and current during CV analysis while immersed in a solution of potassium ferricyanide/ferrocyanide. The ferricyanide/ferrocyanide redox couple was chosen for the relatively small dimensions of these redox active species, which can probe molecular-scale defects in monolayers covering the ITO electrodes.[58] Figure 3.2A includes plots of the 1st, 1,000th and 10,000th CV scans for an RCA-1 cleaned ITO electrode. The RCA-1 cleaned ITO exhibited a subtle decrease in the peak current density (-0.24 mA cm^{-2}) without a significant change in the

oxidation peak position. This decrease in current density was attributed to thermal, photochemical and diffusive based degradation processes of the unmodified ITO interfaces.[1, 15] The CVs obtained for the series of ITO substrates modified with SAMs of ODA, ODTS and ODPA are plotted in Figures 3.2B to 3.2D. All ITO surfaces with or without monolayers, exhibited similar faradaic peak positions after 10,000 consecutive CV scans. This observation indicates most of the electron transports occurs through pin-holes that are separated by a distance greater than the thickness of the diffusion layer at the electrode interface with the solution. This phenomenon has been reported previously with SAMs derived from 1,8-octanedithiol on Au, where the coverage of the SAMs did not lead to a change in peak positons, but led to changes in the current density.[70] The peak current density nominally increased by 0.03 mA cm^{-2} and the peak position changed by -0.01 V over the 10,000 CV scans for ITO electrodes coated with ODA monolayers (Figure 3.2B). During the first positive scan of the electrode potential, the peak current density and position of the oxidation of the ferrocyanide were 1.59 mA cm^{-2} and 0.37 V, respectively. After completing 10,000 scans, the peak current density (1.62 mA cm^{-2}) and its electrochemical potential (0.36 V) remained relatively consistent. Any changes to the CV profiles indicate the degree of molecular-scale changes to the electrode surfaces created during the 10,000 CV scans. The results indicate that the ODA monolayers exhibit high electrochemical and hydrolytic stability under the conditions used in this study. This stability could be attributed to the mechanism by which these monolayers form and the structure of the ODA when covalently bound to the ITO. The hydroxyl group of ODA and terminal hydroxyl groups on the ITO surfaces likely form indium ether (In-O-R) or tin ether (Sn-O-R) linkages through an etherification process. This process could produce monolayers with a chemical structure that is analogous to that of alkanethiols assembled onto gold surfaces.[99] Unlike alcohol based monolayers, this is not the case for ODTS and ODPA derived monolayers.

The silane or phosphonic acid based monolayers can possess multiple chemical structures on the surfaces of the ITO as a result of intermolecular polymerization or a series of varying binding mechanisms.[1] These monolayers are likely to be susceptible to further changes in their structure and surface coverage as a result of oxidation and reduction reactions at the ITO electrodes. Monolayers formed using ODTS initially possessed a similar degree of surface passivation in comparison to monolayers prepared from ODA. The peak current density of the oxidation process for ODTS and its potential

at this peak current were 1.56 mA cm^{-2} and 0.35 V, respectively (Figure 3.2C). During the consecutive scans of the applied potential, the overall magnitude of the oxidation peak decreased and the position of the peak remained consistent. After 10,000 CV scans, the oxidation peak current density decreased to 1.25 mA cm^{-2}, corresponding to an overall reduction of 0.31 mA cm^{-2}. This decrease in peak current density is attributed to restructuring of the ODTS coating. Previous studies demonstrated the susceptibility of silane based monolayers to thermal, chemical and hydrolytic damage.[42, 87, 100] Thin silicon oxide films also have been produced from silanes through intermolecular polymerization and hydrolysis of the Si-C bonds.[92] In addition, Si-C bonds are more susceptible to hydrolysis as they exhibit a weaker bond strength than Si-O bonds.[101] We hypothesize that the ODTS monolayers decomposed to form thin silicon oxide films on the ITO surfaces through a process of electrochemical, chemical, and hydrolytic stresses. This additional passivation increases the resistivity at the interface between the ITO and the electrolytes. Monolayers prepared from ODPA initially demonstrated a very high degree of surface passivation with a relatively low oxidation peak current density (0.69 mA cm^{-2}) and a relatively high oxidation peak potential (0.50 V). Significant changes in both the peak current density (+0.65 mA cm^{-2}) and the position of the oxidative peak potential (-0.13 V) were observed after 10,000 scans of the applied potential (Figure 3.2D). These significant changes to the oxidative conditions of the ferricyanide/ferrocyanide redox couple are attributed to restructuring of the ODPA coatings. The phosphonic acids interact through three distinct denticities with the ITO surfaces, and structural changes can induce changes in their binding denticity.[28] In addition, it has been shown that In-O-P bonds can be easily hydrolyzed when exposed to moisture.[48] The restructuring of the ODPA coatings likely leads to the dissolution of individual ODPA molecules, leaving defects within the monolayers on the ITO surfaces. These changes could significantly compromise the electronic properties of the modified ITO substrates. Additional studies were performed to further assess these structural changes to the monolayers including dissolution of bound species.

Water contact angle studies can be used to estimate the surface coverage of monolayers.[59] In this study, changes in WCA values were used to infer changes in their surface coverage. The WCA values for all of the as-prepared and electrochemically tested monolayers, as well as the RCA-1 cleaned ITO, were assessed for changes to their surface passivation. The WCA values were obtained from 8 different areas within each

sample and there were some variations in the volumes of each of the water droplets due to changes in the environmental conditions. The RCA-1 cleaned ITO electrodes initially exhibited a WCA value of ~0° and after repeated electrochemical tests the WCA increased to ~9°. This increase in WCA is attributed to an increase in the surface coverage of O-In-O bonds through condensation of In-OH bonds, accumulation of organic contaminants, or leaching of indium species from the surfaces that could expose an underlying layer of oxygen deficient In.[1, 89, 102] The WCA values for each of the as-prepared monolayers on the ITO electrodes were consistent. The ODA coated substrates exhibited average WCA values of ~100 ± 4°, while ODTS and ODPA coated substrates exhibited average WCAs of ~112 ± 10° and ~102 ± 7°, respectively (Figure 3.3). After the electrochemical experiments, changes to the average WCAs for the ITO substrates coated with ODA, ODTS, and ODPA were -3°, -13°, and -20°, respectively (Figure 3.4). The changes in WCAs observed for the ODPA monolayers agrees well with observations made in our electrochemical stability experiments. These results are also consistent with the hydrolytic sensitivity of ODPA reported in the literature.[48] These changes are attributed in part to a change in the binding states of the ODPA molecules, which can result from exposure to moisture through hydrolysis of In-O-P bonds.[48] The WCA results further support the conclusions that as a result of the electrochemical tests and their hydrolytic conditions the silane molecules experienced structural changes and the phosphonic acid molecules likely undergo dissolution from the ITO surfaces. A matched pair t-test was performed to assess the statistical significance of the observed changes in the WCA values. The test indicated that the changes observed for the ODA coated ITO had a 95% statistical significance [degree of freedom (df) = 7 and t = 1.96] between the values measured before and after the electrochemical tests. The ODTS coated ITO and the ODPA coated ITO substrates, on the other hand, exhibited a 97.5% significance (df = 7, and t = 2.70 and 2.77, respectively) in the observed change in average WCA value. To confirm that the changes in the WCA did not originate from change in surface morphology, atomic force microscopy (AFM) measurements were obtained for the unmodified and modified ITO substrates. The AFM measurements obtained after the CV analyses indicated that the surface roughness of the ITO substrates modified with monolayers derived from ODA and ODPA remained relatively consistent with the observed roughness for the RCA-1 cleaned ITO (Figure 3.5). Surface roughness of the ITO substrates modified with ODTS did, however, exhibit a decrease of ~2 nm (Table 3.1).

$$H = \theta_a - \theta_r$$ *Equation 3.1*

To further assess the quality of the alcohol based monolayers, 5 advancing contact angles and 4 receding contact angles were measured on an ODA coated ITO substrate from 2 different regions. The hysteresis values were calculated according to the relationship in Equation 3.1. The hysteresis measured for the two locations was 20.4° and 13.5°. This significant hysteresis in the WCA values indicates that the surfaces are not homogeneous, which is likely a function of both the surface coverage of these SAMs and the surface roughness of these substrates. In addition, the ODA coated ITO substrates were exposed to either 1 M KCl solution or 1 M KCl solution containing 10 mM of ferricyanide/ferrocyanide redox couple for the same period of time required for each of the CV analyses (~2.5 days). Potential degradation of the monolayers was assessed through calculating the change in WCA values from the original values prior to immersion in these solutions. These WCA measurements were obtained from 4 different regions of the substrate with negligible (~0°) change from the original values. The result of this study further indicate that the electrochemical tests accelerate the hydrolysis of the monolayers. Specific changes to the chemical composition of each interface required further analysis to better understand the observations made regarding the stability of all prepared monolayers.
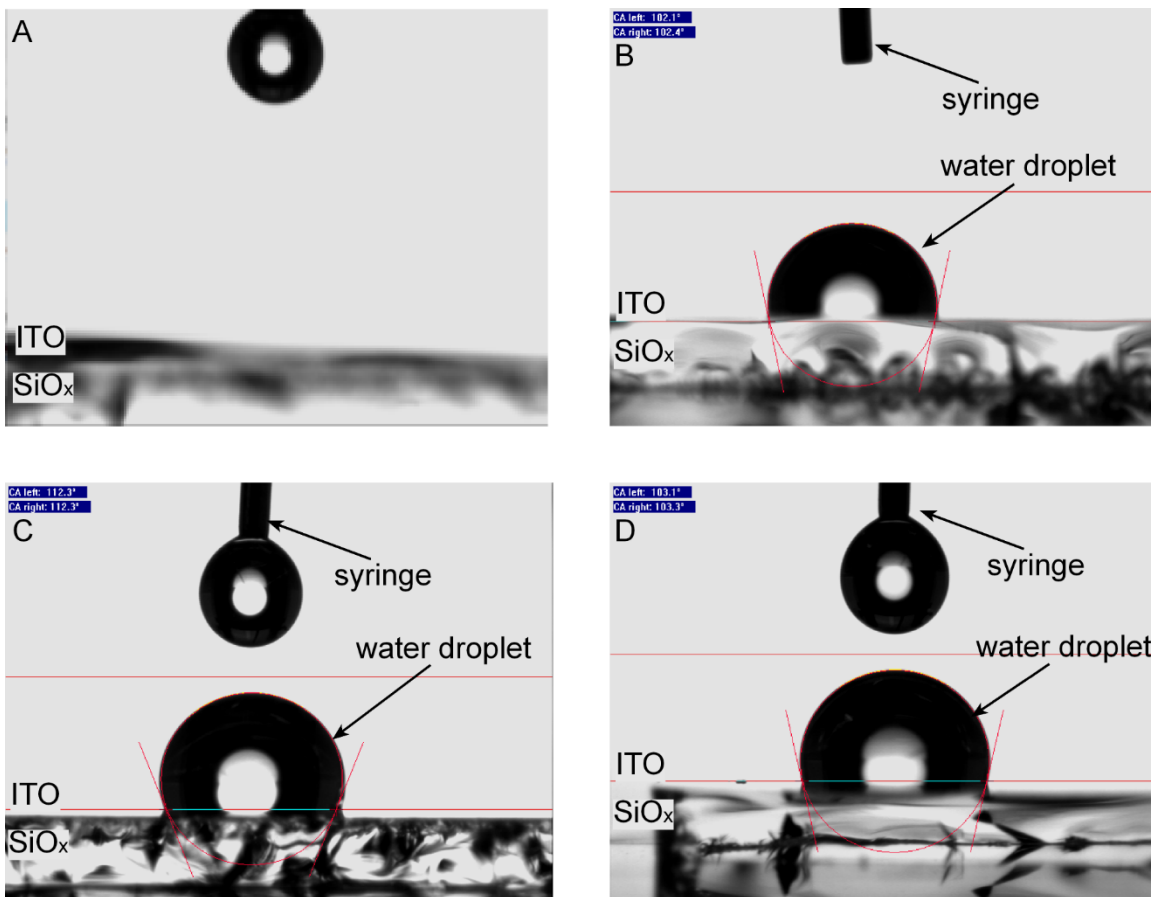
Figure 3.3   **Representative WCA measurements for: (A) RCA-1 cleaned ITO; (B) ODA coated ITO; (C) ODTS coated ITO; and (D) ODPA coated ITO substrates.**
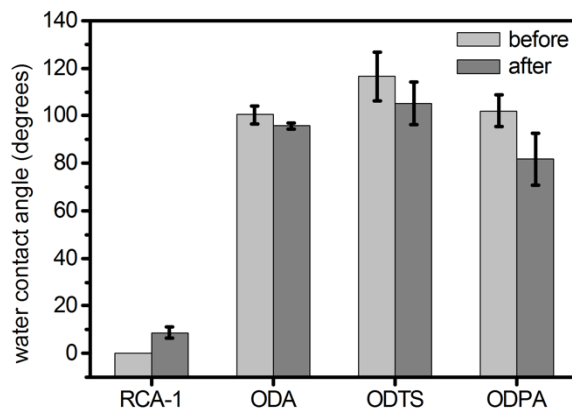
Figure 3.4   **Water contact angles (WCAs) of RCA-1 cleaned ITO and ITO modified with either ODA, ODTS, or ODPA. These average WCA values were calculated using measurements from 8 independent regions on each sample, which were obtained either before or after the series of electrochemical and hydrolytic tests as noted in the legend.**
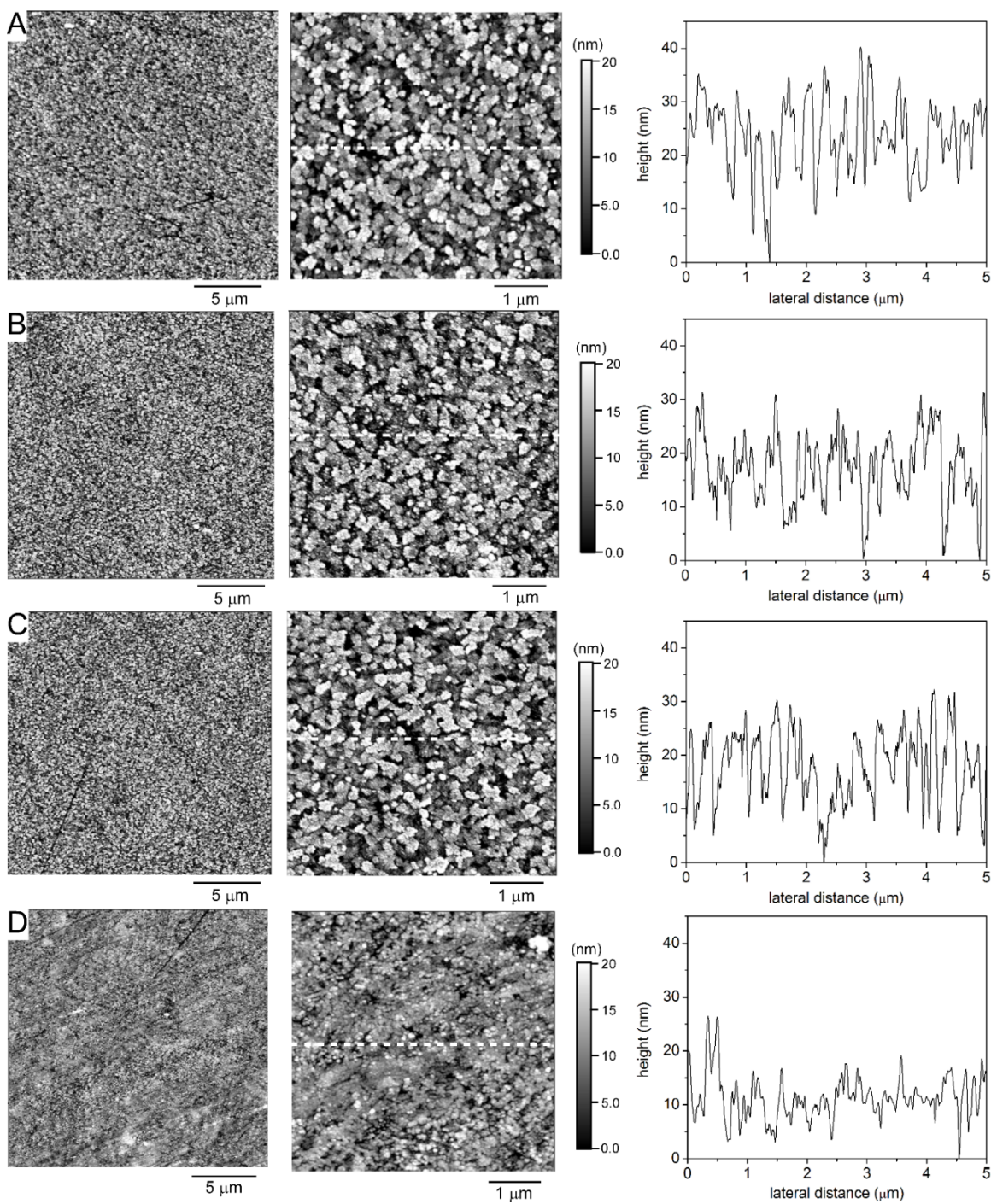
Figure 3.5 **Atomic force microscopy (AFM) images of modified surfaces after CV analyses: (A) RCA-1 cleaned ITO; (B) ODA coated ITO; (C) ODPA coated ITO; and (D) ODTS coated ITO.**

Table 3.1   **Root mean square (RMS) roughness values from AFM measurements for unmodified and modified ITO substrates.**

ITO treatment or surface modification	RMS (nm)
RCA-1 cleaned	6.11
ODA	6.62
ODPA	6.03
ODTS	4.13

To accurately measure changes in the composition of each interface, the surfaces of the ITO substrates were analyzed by XPS. High resolution XPS analysis of the O_{1s} peaks (Figure 3.6) were monitored before and after the electrochemical experiments. The O_{1s} species were selected as the molecules within the monolayers are anticipated to interact with the ITO through oxygen bonds (e.g., In-O-C, In-O-P and In-O-Si).[28, 51] Three O_{1s} peaks were observed for each of the substrates, which were attributed to O-In-**O**H, **O**-In-O and **O**-C at binding energies of 529.5 eV, 530.4 eV and 531.5 eV, respectively. All of the three oxygen species are present at the surfaces, as commercially available ITO are often amorphous or polycrystalline. The same peak positions for these peaks were previously reported in the literature.[3, 12, 27, 33, 84] The peak area ratio between O-In-**O**H and **O**-In-O maintained a value of approximately at 2 for all of the samples. The binding energies of the oxygen atoms within the silane or phosphonic acid based monolayers (**O**-Si, **O**-P or **O**=P) overlapped with the **O**-C peak position. A shift in the binding energy for the **O**-C species was observed after preparation of the monolayers when compared to the RCA-1 cleaned ITO substrates. This shift was attributed to a shift in the Fermi level (E_F) at the interface between the ITO and the monolayers. When comparing the XPS spectra before and after the extended electrochemical tests, no significant changes in composition were observed for the RCA-1 cleaned ITO substrates (Figure 3.6A) or the ODA coated

ITO (Figure 3.6B). The XPS spectra obtained from ODA monolayers before and after the CV analyses suggest that the changes in the chemical composition of the ITO surfaces were minimal for these substrates after extended electrochemical and hydrolytic testing. In contrast, significant spectral changes were observed for the substrates coated with either ODTS or ODPA. For the ODTS coated ITO, significant changes in the intensity of the **O**-Si species were observed from the XPS analysis. After repeatedly cycling the applied potential, the spectrum exhibited a significantly reduced intensity of the **O**-Si species in comparison to the O-In-**O**H and **O**-In-O species (Figure 3.6C). This change was attributed to the formation of a multilayer structure within the as-deposited ODTS and the subsequent loss of non-covalently attached ODTS molecules and/or degradation of the monolayers of ODTS. The ODPA coated ITO substrates also exhibited a significant change in their high resolution XPS spectra when comparing the plots obtained before and after the extensive electrochemical testing. Initially, the high resolution O_{1s} spectrum for the ODPA monolayers exhibited similar peak intensities to those observed for the RCA-1 cleaned ITO surfaces. After evaluating the electrochemical stability of the ODPA monolayers, the peak intensity of the O-In-**O**H species significantly decreased relative to the **O**-C or **O**-In-O species (Figure 3.6D). This phenomenon was attributed to etching or non-specific degradation of the underlying ITO films. The ODPA monolayers likely underwent restructuring and degradation from electrochemical and hydrolytic stresses. One example is the hydrolysis of the In-O-P bonds, which produces H_3O^+ and increases local acidity.[48] Another example is that weakly bound In or Sn atoms coordinate with phosphonic acids and undergo complexation to form an insoluble salt.[16, 103] Previous studies reported changes in the relative content of In and Sn on the surfaces of ITO due to etching of In with an acid.[85, 104] Another study proposed that phosphoric acid slowly etches ITO and could be used to extract In species from solution.[48, 105] The results of these XPS analyses confirmed the observations made from the CV and WCA analyses, which suggested changes to the chemical composition and structure of the ODTS and ODPA monolayers upon prolonged electrochemical and hydrolytic testing. In summary, the ODA coated ITO demonstrated a greater electrochemical and chemical stability in contrast to ODTS or ODPA coated ITO. The ODA monolayers on ITO could serve as an alternative passivation layer for fine tuning the surface properties of ITO for a variety of applications, such as displays, touchscreens, heat reflective coatings and smart windows.[1, 12, 16] Evaluating these coatings for their potential use in optoelectronic devices required a

further assessment of possible changes to their optical properties.
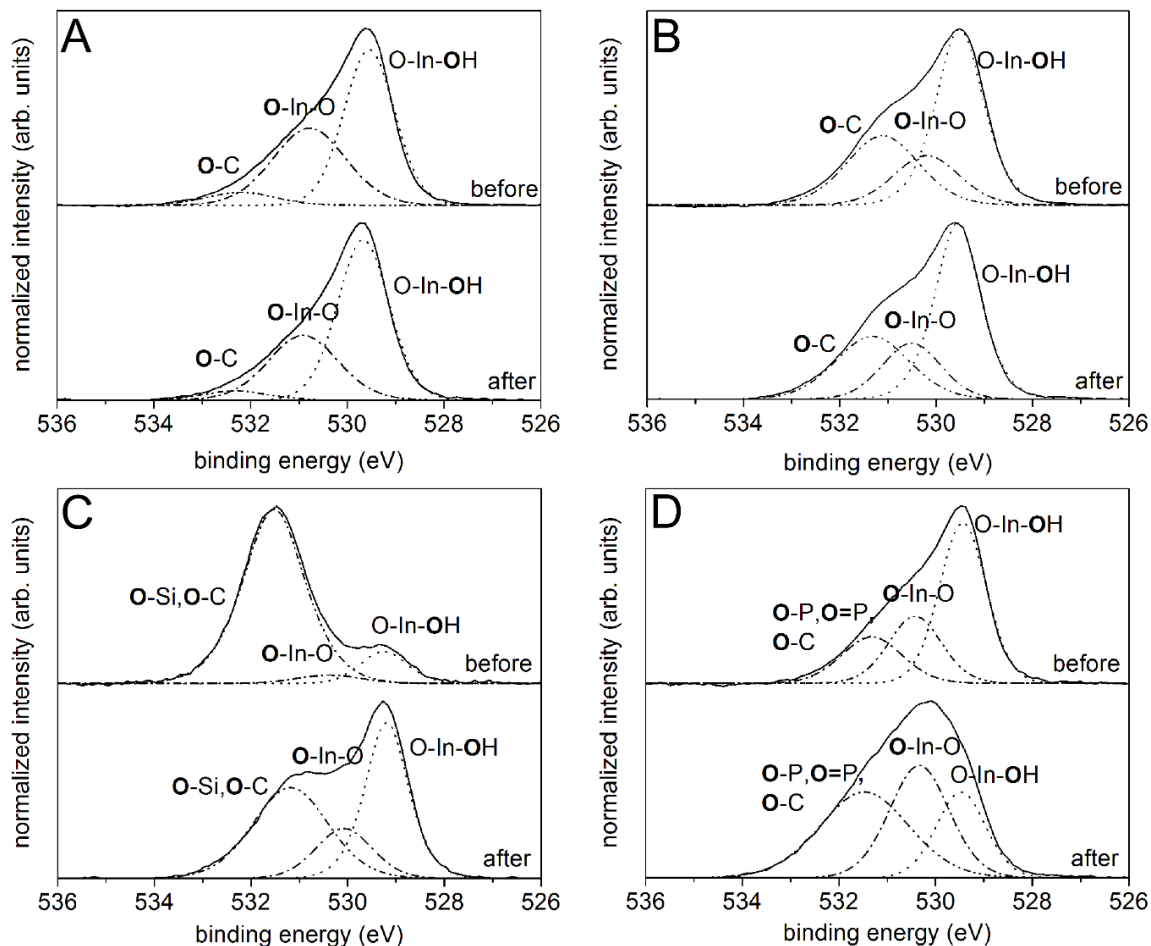
Figure 3.6 **High resolution XPS data for O_{1s} species associated with: (A) RCA-1 cleaned ITO; (B) ODA coated ITO; (C) ODTS coated ITO; and (D) ODPA coated ITO. Representative spectra are plotted for each type of surface modification, which were obtained either before or after the series of electrochemical experiments as noted above each plot.**

3.3.2. Optical Properties of Organic Monolayers on ITO

The optical properties of the modified ITO films were evaluated after repeated electrochemical and hydrolytic testing. The optical transmittance of these substrates was evaluated using UV-Vis transmission spectroscopy. Specifically, transmittance between 350 and 750 nm was investigated to monitor changes in the desired optical properties of the ITO films. Substrates coated with monolayers of either ODPA or ODA did not exhibit any spectral shift in comparison to the RCA-1 cleaned ITO substrates (Figure 3.7). A blue shift was, however, observed for the ODTS modified ITO after electrochemical testing.

This phenomenon is attributed to deformation of the ODTS coatings in to a thin SiO_x film. The additional SiO_x layer leads to a change in the optical dielectric properties of these interfaces, which alters the position of the interference pattern observed in the UV-Vis transmission spectra.[106] Previously, thin films of silicon oxide prepared from the decomposition of tris-dimethylaminosilane exhibit a similar UV-Vis transmission spectrum.[92] Decomposition of silane based monolayers, such as through the formation of silicon oxide, could induce the observed changes in the transmittance properties of the ITO films. It is speculated that the blue tint observed for the ODTS coatings was due to the formation of a thin silicon oxide layer. This change in the dielectric properties at the ITO surfaces could lead to the shift in the features observed within the transmission spectrum.[106] Figure 3.8 shows the visible blue tint of the ODTS coated ITO films after 2.5 days of continuous evaluation of their electrochemical and hydrolytic stability. Within this film, the corners and edges exhibited a more vivid blue coloration. Non-uniformities in the current density between the edges and center of the ITO electrodes could lead to this differential growth of the silicon oxide films.[107] The monolayers prepared from phosphonic acids or aliphatic alcohols did not show any significant change in their optical transmittance properties.
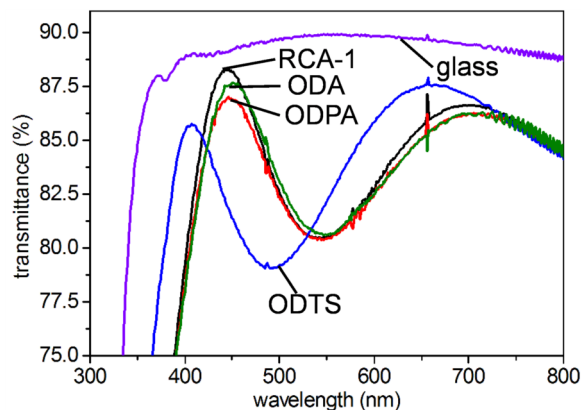
Figure 3.7   **Ultraviolet-visible (UV-Vis) transmittance spectra of RCA-1 cleaned ITO, ODA coated ITO, ODTS coated ITO, ODPA coated ITO, and glass slide obtained after a series of electrochemical and hydrolytic tests.**
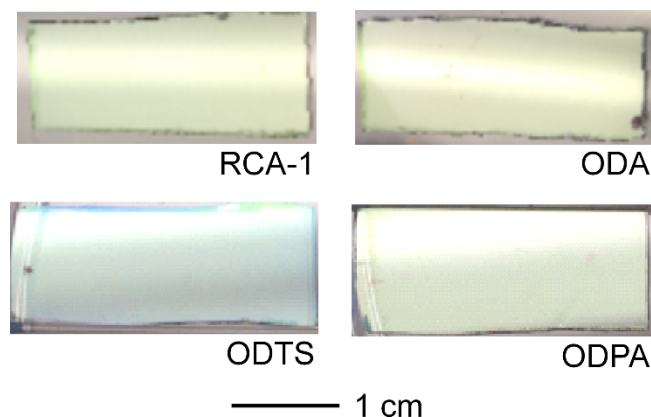
Figure 3.8   **A blue tint was observed for the ODTS modified ITO substrates in comparison to RCA-1 cleaned, ODA coated and ODPA coated ITO substrates after the prolonged electrochemical tests.**

3.3.3.   Electronic Properties of Alcohol Based Monolayers on ITO

To evaluate the utility and electronic properties of alcohol based monolayers in organic electronics, their surface energy and work function must be determined to assess their compatibility with the HTL.[5] Previous studies demonstrated that incompatibilities can lead to a non-uniform wetting of the non-polar organic HTL.[25, 27, 47] In OLEDs and OPVs, a mismatch in these two properties between ITO and the HTL must be minimized to optimize their electronic performance. The modification of ITO with SAMs can be used to reduce the surface energy of this interface and to establish a stable interfacial chemistry. For example, a higher luminance at fixed potentials was achieved through the use of silane based monolayers on ITO in comparison to unmodified ITO.[5] This result was attributed to improvements in the uniformity of the thickness and wetting of the HTL on the ITO substrate. As surface energy of the ITO can be an indication of the uniform wetting of the HTL, it is important to determine the surface energy of modified ITO surfaces. This assessment can indicate the utility of various monolayers for use in organic based electronic devices.

Surface energies of the monolayers on the ITO substrates were derived using the Owen-Wendt model of wetting, which can be used to estimate the total surface energy.[74] The Owen-Wendt model (Equation 2.6) can also be used to derive the polar and dispersive components of the surface energy of the ITO substrates. In this equation, θ_c represents the contact angle of the liquid interest and γ is the surface tensions. The subscripts *LV* and

50

SV represent the liquid-vapor and solid-vapor interactions, respectively, while the superscripts *d* and *p* represent dispersive and polar components.[74] The Owen-Wendt model requires contact angle measurements to be obtained using two distinct liquids. In this study, water and n-hexadecane contact angles were used to derive the polar and dispersive components of the surface energy, as well as the total surface energy of each sample. For all of the substrates, at least four independent contact angle measurements were obtained using each of the liquids. The results of these contact angle measurements are summarized in Table 3.2. The RCA-1 cleaned ITO sample exhibited contact angle values of ~0° for both water and n-hexadecane. Based on these measurements, the total surface energy of the RCA-1 cleaned ITO was calculated to be 73 mJ m^{-2}, and the polar and dispersive components were 46 and 28 mJ m^{-2}, respectively. Monolayers derived from ODA, ODTS, and ODPA exhibited consistent values for their total surface energy (e.g., 23 to 27 mJ m^{-2}). These results are significantly lower than those for the RCA-1 cleaned ITO substrates. The lower surface energies of the modified ITO would enable a more uniform wetting of the HTL. Previous studies have reported values of 29 mJ m^{-2} for monolayers of ODPA and ODTS.[27, 29] These lower surface energy values are important to achieve the desired efficiencies and lifetimes of OLEDs and OPVs.[34] Other alcohol reagents were also evaluated to better understand the ability to tune the surface energy through altering the composition of the alcohol based monolayers.

Composition of the alcohol based monolayers derived from alcohol species were tuned between two extremes. One type of reactant was a perfluorinated species (i.e., 1*H*,1*H*,2*H*,2*H*-perfluoro-octanol or PFOA), and the other species were linear diols (i.e., 1,5-pentanediol or PTdiA and 1,10-decandiol or DCdiA). These substrates exhibited slightly higher total surface energies than the linear hydrocarbon chains (Table 3.2). The estimated surface energies were 34, 48 and 46 mJ m^{-2} for PFOA, PTdiA and DCdiA, respectively. The total surface energies for each of these monolayers, along with a distinction of their polar and dispersive components, are graphically depicted in Figure 3.9. The variation in surface energies observed for the different alcohol based reagents indicate that the composition of these monolayers can be tuned to sufficiently adjust the surface energy. This tunability could be necessary to create a compatible interface for uniform wetting of different HTLs. Modifications to the ITO surfaces also result in changes to their surface work function, which can lead to further improvements in device performance.

Table 3.2   Average contact angle values for the ITO substrates and their corresponding surface energies derived using the Owen-Wendt model of wetting.

ITO treatment/modification	water θ^*	n-hexadecane θ	γ, polar component[‡] G	H	γ, dispersive component G	H	γ, total G	H
RCA-1 cleaned	0 ± 0	0 ± 0	46	46	28	28	73	73
ODA	100 ± 2	13 ± 2	0.6	0.55	27	27	27	27
ODTS	111 ± 7	19 ± 3	0.021	1.7E-3	26	26	26	26
ODPA	102 ± 7	33 ± 4	0.062	3.3E-5	23	23	23	23
PFOA	75 ± 4	31 ± 3	11	10	24	24	34	34
PTdiA	55 ± 2	5 ± 1	21	21	27	27	48	48
DCdiA	58 ± 1	9 ± 2	19	19	27	27	46	46

* = Average contact angle (degrees).
‡ = Surface energy (mJ m^{-2}), G = geometric mean, and H = harmonic mean.
Standard errors in contact angle measurements were $\leq 2°$.
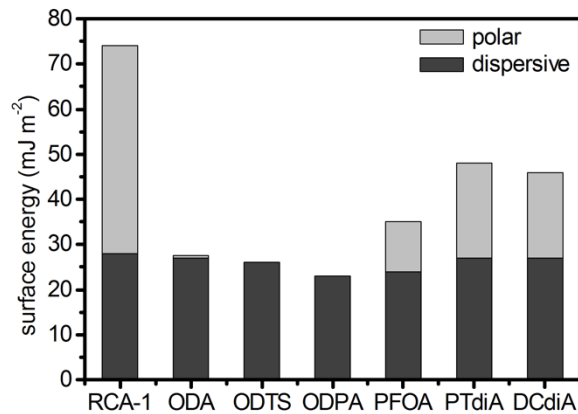
Figure 3.9   Surface energies derived using the Owen-Wendt model of wetting for RCA-1 cleaned ITO and ITO coated with ODTS, ODPA, ODA, 1H,1H,2H,2H-perfluoro-octanol (PFOA), 1,5-pentanediol (PTdiA) and 1,10-decandiol (DCdiA). The polar and dispersive components of the surface energy are represented by the light grey (upper) and dark grey (lower) columns, respectively.

The work function of ITO electrodes at the interface with potential HTL can be adjusted using SAMs. There is a significant mismatch in work function between the native ITO and the HTL.[1-2, 25-27, 29, 51, 62] This mismatch is often referred as hole transport barrier. The larger the barrier is, the higher is the required energy to operate the device. Monolayers can be used to effectively tune the work function of metals and semiconductors, while increasing the efficiency of the hole injection process.[29, 34, 51] These

achievements result from the creation of a new permanent surface dipole. Ultraviolet photoelectron spectroscopy (UPS) measurements can be used to determine the work function of materials.[79, 102, 108] Previous UPS studies compared the work functions of monolayers of n-alkylphosphonic acid and other phosphonic acids on ITO to those of triton X-100 cleaned ITO and oxygen plasma treated ITO.[26-27, 34] The triton X-100 cleaned ITO had a work function of 4.6 eV, and that for the oxygen plasma treated ITO was 5.1 eV.[27, 102] The n-alkylphosphonic acid monolayers decreased the work function of ITO by 0.6 eV, while other phosphonic acids, such as fluorinated and phenylated phosphonic acids, exhibited equal or higher work functions in comparison to the oxygen plasma treated ITO. These results indicate that work functions can be tuned through the use of various terminal groups within the monolayers. The work functions of a series of ITO substrates, each modified with different alcohol based monolayers, were determined through UPS measurements. Work functions of the alcohol based monolayers were compared with RCA-1 cleaned ITO, as well as to ITO substrates modified with either alkylsilanes or alkylphosphonic acids.

Alcohol based monolayers were specifically evaluated for their ability to tune the work function of ITO. This study included SAMs prepared from ODA, PTdiA, DCdiA, and PFOA. Three separate measurements were obtained from different regions of each substrate to assess the regularity of each work function. Important information extracted from the UPS spectra included the width of the spectrum, or the range between the secondary electron edge and the Fermi level or E_F (0 eV).[1, 11, 27, 51, 102, 108] The difference between the width of the UPS spectrum and the energy of the helium 1 source (e.g., 21.2 eV) was used to determine the work function of the RCA-1 cleaned ITO film (4.73 eV). This value was similar to those reported in the literature for clean ITO, which range from 4.5 to 4.7 eV.[25-27, 29, 51, 108] Monolayer modified ITO surfaces required a more detailed assessment of the energy levels and their shifts for an accurate determination of their work functions.

An accurate determination of the work function of the monolayer modified surfaces requires the consideration of both band bending and shifts in E_F.[14, 27, 81, 83] Band bending occurs through E_F pinning at the interface of two different materials. This phenomenon decreases the work function of ITO, resulting in an increase in the hole-injection barrier when ITO is used as the anode in electronic devices. Monolayers exhibit a permanent

53

surface dipole moment that can shift the vacuum level (E_{vac}) and either increase or decrease the work function depending on the overall direction of the dipole.[4, 11, 14, 27, 81, 83] There are two components in determining the overall direction of the dipole: (i) the induced dipole at the interface between the ITO and the monolayers, and (ii) the permanent dipole of the molecular constituents of the monolayers.[81] Depending on the overall direction of the dipole, the energy levels are shifted either upward or downward. For example, monolayers prepared from molecules with a negative dipole oriented away from the ITO can raise the level of E_{vac}, increasing the local work function of the electrode. This shift in the energy level of E_{vac} can offset a decrease in work function that results from band bending.[81, 83] The overall shift in the energy levels from the contributions of the surface dipole and band bending can be measured by monitoring the position of valence band maximum (VBM) and secondary electron edge in the UPS spectrum. The onset of the electronic transitions (at ~3 eV) observed for the monolayers on ITO is compared to that measured for the RCA-1 cleaned ITO to estimate the relative shift in each spectrum. The width of the UPS spectra, after accounting for these shifts, were used to more accurately compute the work functions of the modified ITO substrates.[4, 11-12, 27] The reported work function values for ODTS and ODPA monolayers on ITO are 4.85 eV and 4.5 eV, respectively.[27, 29] Our coatings prepared from ODTS and ODPA exhibited work function values of 4.07 eV and 4.78 eV, respectively. The previously reported value for ODTS modified ITO films did not account for the shift in E_F and band bending, which resulted in a higher value than derived from our measurements. In addition, this value was measured using Kelvin probe, which measurements can be influenced by obtaining measurements under ambient atmospheric conditions (e.g., adsorbed water layers or other species).[14, 108-109] Monolayers derived from ODA on ITO exhibited a work function of 4.74 eV, which is close to the value for ODPA monolayers on ITO. In electronic devices that utilize ITO as an anode, a high work function for the ITO electrode (e.g., ≥ 5 eV) is desired to minimize the hole injection barrier, which is sought to improve the performance and lifetime of these devices. Although these measurements indicate that alcohol based monolayers are comparable to monolayers derived from alkylsilanes and alkylphosphonic acids, the work function of the ODA coated ITO was not significantly improved in comparison to RCA-1 cleaned ITO.
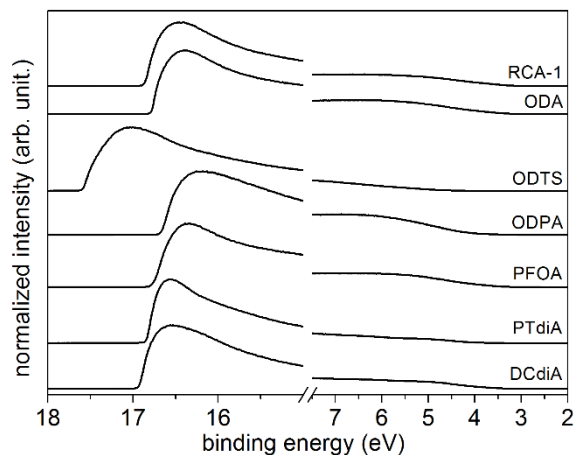
Figure 3.10 **The UPS spectra of RCA-1 cleaned ITO and the series of ITO substrates modified by SAMs, which are indicated above each spectrum. These spectra are plotted to depict the secondary electron edge and the Fermi levels (E_F) associated with each of these substrates.**

A high work function can be achieved through tuning the terminal functional groups within SAMs. Based on previous studies, electron withdrawing groups can be incorporated into SAMs to increase the work function because of their higher electron affinity in comparison to alkyl chains.[25-26, 34, 81] The work functions of ITO modified with PTdiA, DCdiA and PFOA were determined using the methods described above. Figure 3.10 depicts the UPS spectra for each of the samples that were normalized to the maximum peak intensity. The computed average work function values with errors reported to one standard deviation are summarized in Table 3.3. The work functions for the ODA, PTdiA, DCdiA and PFOA monolayers were 4.74 eV, 4.58 eV, 4.49 eV and 4.88 eV, respectively. Treatments with either of the diols, PTdiA or DCdiA, decreased the work function by 0.15 and 0.24 eV, respectively, in comparison to the RCA-1 cleaned sample. This decrease was attributed to the difference in magnitude of the dipoles between the In-O-H and C-O-H terminated surfaces. To increase the work function, a surface dipole created by the monolayers must be larger than the dipole of the native surfaces. The ITO surfaces include both polar oxo and hydroxyl groups (e.g., In-O-In and In-O-H). A previous study reported a similar phenomenon with pentafluorobenzyl phosphonic acid, which exhibited a lower work function than anticipated for this species. This decrease in work function was attributed to the fluorine atoms on the phenyl ring, where all of the dipoles formed by each of the fluorine atoms were cancelled one another, except for the fluorine at the para position.[27]

The PFOA sample was the only alcohol based monolayers that exhibited a work function that was higher than the RCA-1 cleaned sample. A similar result was previously reported with fluorinated phosphonic acid species used to prepare monolayers on ITO. Monolayers derived from 3,3,4,4,5,5,6,6,7,7,8,8,8-tridecafluorooctyl phosphonic acid exhibited a work function that was equal to the oxygen plasma treated ITO.[27] These results indicate that the fluorine moiety of the monolayers creates a stronger surface dipole than hydrocarbons and can, therefore, increase the work function. The range of values in work function demonstrated for the alcohol based monolayers suggest that the work function of ITO can be tuned using different alcohol reagents. This study demonstrated the preparation of ITO coated with monolayers derived from alcohol based reactants with potential use in organic based electronic devices, such as OLEDs and OPVs, through designing the ITO interface to exhibit the desirable surface energy and work function.

Table 3.3   Work functions obtained from UPS spectra (He 1 Source).

sample	work function (eV)
RCA-1 cleaned	4.73 ± 0.20
ODA	4.74 ± 0.27
ODTS	4.07 ± 0.05
ODPA	4.78 ± 0.26
PFOA	4.88 ± 0.08
PTdiA	4.58 ± 0.13
DCdiA	4.49 ± 0.16

3.3.4.   Varying the Hydrocarbon Chain Length for Alcohol Based Monolayers on ITO

An important property of monolayers attached to ITO films is their influence on the current passed through this interface as part of an electrochemical device.[97-98] We studied the relationship between the electrical properties of these alcohol based monolayers on ITO and their chain length. A series of electrochemical studies were performed with the modified ITO substrates while monitoring the peak current passed through the monolayers. A series of molecules with an even number of carbons in their backbone were selected for these experiments to eliminate the possibility of odd-even effects observed in the packing density and electronic properties of some types of monolayers.[60, 63, 110] We evaluated the degree of change in the current passed through the monolayers over the

course of the electrochemical studies. We specifically monitored the peak faradaic current. The most significant peak shifts were observed within the first 1,000 scans of the applied potential. Peak positions were, therefore, reported at the 1,000[th] scan. Hydrocarbon chain length and peak current exhibited a linear correlation (Figure 3.11). Every two additional carbons in the backbone of the monolayers exhibited an average decrease of ~0.18 mA cm^{-2} in the peak faradaic current density or ~0.027 log $|J|$ at the faradaic peak. A similar relationship has been observed in a study on thiol based monolayers on Au surfaces.[60, 63, 111] Varying the hydrocarbon chain length of phosphonic acids on SrTiO$_3$ have also shown a similar relationship.[112] The length of the hydrocarbon chain was directly correlated with the observed peak current density recorded for the modified ITO films. For reference, the 1,000[th] CV profiles of each sample is shown in Figure 3.12. The peak faradaic current for the modified ITO can be tailored by choice of the appropriate reagent. In summary, the monolayers prepared on the ITO surfaces can be used to design their electronic properties for the needs of specific organic based devices.[49]
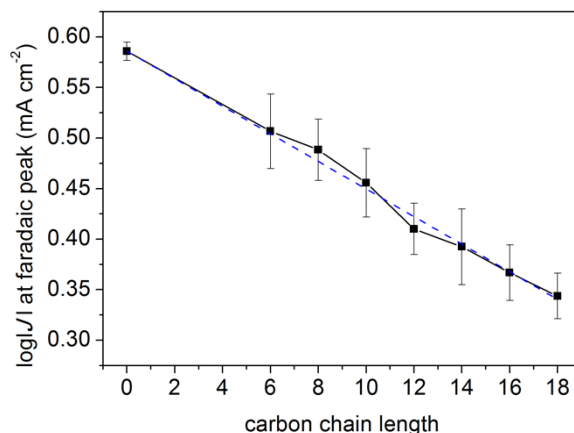
Figure 3.11   Average Log $|J|$ values obtained at faradaic peaks from CV experiments carried out for ITO substrates coated with a series of monolayers. Data were obtained at a 200 mV s^{-1} scan rate. The reported peak current densities are each an average from the measurements of three independent samples. These measurements were taken after the 1,000[th] scan of the applied potential for each of the modified ITO electrodes. Each of the monolayers were prepared from linear aliphatic alcohols of the specified chain length, as indicated on the x-axis. The dashed line is a linear fit to the observed and the error bars for each data point indicate one standard deviation from the mean values.
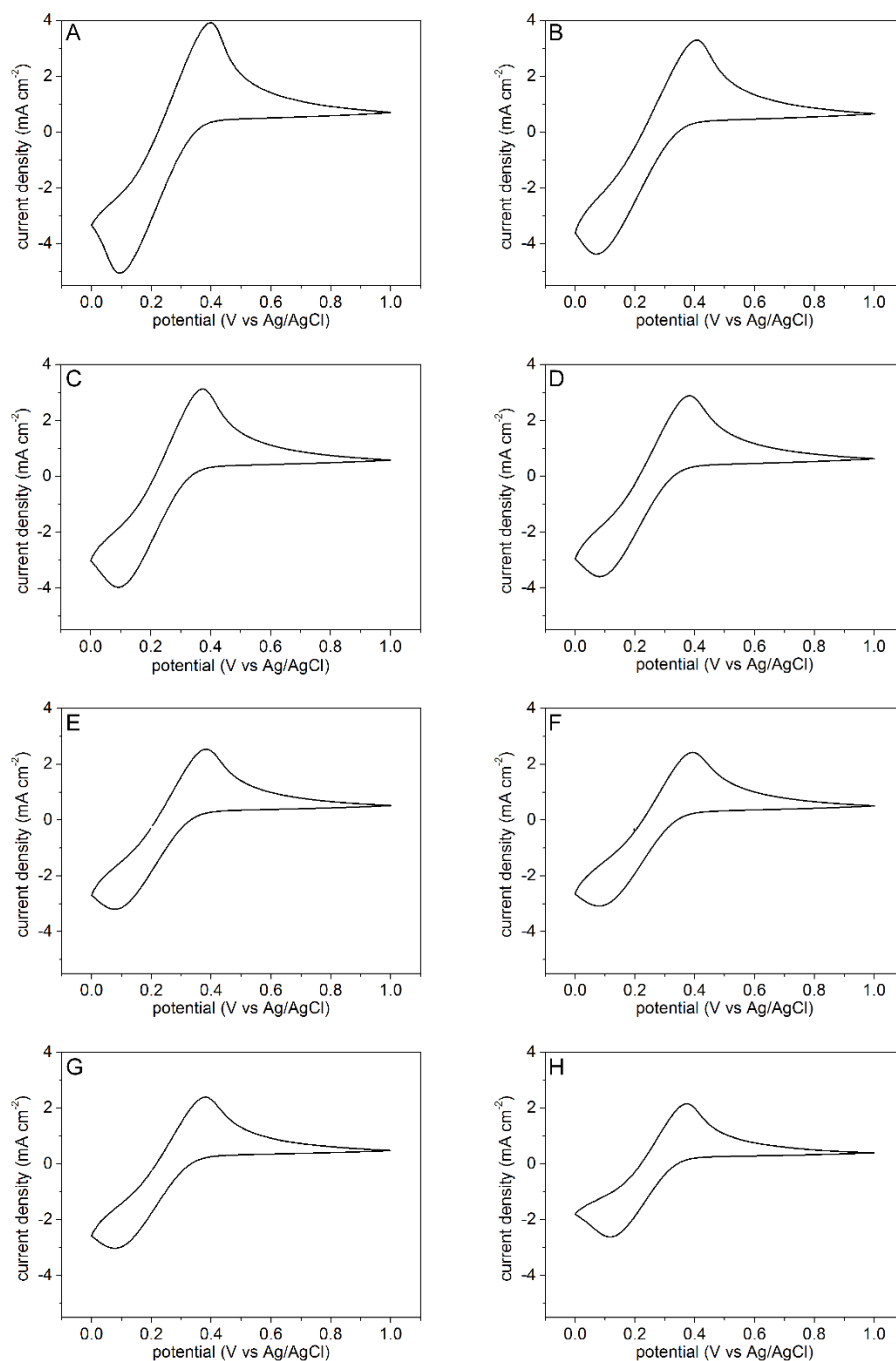
Figure 3.12 The 1,000th profile from a consecutive series of cyclic voltammetry analyses for: (A) RCA-1 cleaned ITO; (B) 1-hexanol coated ITO; (C) 1-octanol coated ITO; (D) 1-decanol coated ITO; (E) 1-dodecanol coated ITO; (F) 1-tetradecanol coated ITO; (G) 1-hexadecanol coated ITO; and (H) 1-octadecanol coated ITO. These electrochemical studies were carried out at a scan rate of 200 mV s^{-1} using the ITO substrates as the working electrode in 1 M KCl solutions containing 10 mM of potassium ferricyanide and 10 mM of potassium ferrocyanide.

3.4. Conclusions

The modification of ITO surfaces with self-assembled monolayers have been used to tune the properties of the ITO for use in a variety of organic based electronic devices. Herein, a new class of monolayers on ITO, alcohol based monolayers, have been demonstrated for the first time. Several different alcohol containing reagents were successfully grafted onto ITO surfaces through a condensation reaction to form covalent bonds. The electrochemical analyses of these alcohol based monolayers on ITO by CV techniques demonstrated their electrochemical and hydrolytic stability, in a direct comparison to surfaces modified with silanes or phosphonic acids. Alcohol based monolayers exhibited a change of only 0.03 mA cm^{-2} and -0.01 V in the faradaic peak current density and peak position after a series of continuous stability tests each carried out over the course of ~2.5 days. The notable stability of the alcohol based monolayers relative to monolayers of silanes or phosphonic acids was further confirmed through WCA measurements and XPS analyses. The optical transmittance of the alcohol based monolayers on ITO exhibited minimal changes after these stability tests. In contrast, the silane based monolayers exhibited a notable degradation in film quality as observed by both electrochemical and optical techniques. In addition, electronic properties of each of the monolayers, which include their surface energy and work function, were analyzed using the Owen-Wendt model of wetting and UPS techniques. The surface energy was tuned from 27 to 48 mJ m^{-2} and the work function adjusted from 4.49 to 4.88 eV through changes to the composition of the alcohol based monolayers. These results indicated that the alcohol based monolayers can simultaneously modify both the surface energy and work function of the ITO. This approach to modifying ITO is a promising technique for adjusting the properties of the ITO for its use in organic based electronic devices. The alcohols based monolayers on ITO exhibited an exceptional electrochemical and chemical stability that is required for their prolonged use in electronic devices. In addition, these surface modifications to ITO can readily incorporate a terminal hydroxyl moiety through the use of diols. These hydroxyl groups could potentially provide a platform for further chemical reactions and for applications in electronic devices other than OLEDs and OPVs, such as molecular sensors and organic transistors.

3.5. Experimental

3.5.1. Reagents for Pretreatment of ITO

All reagents and materials were used as received, which include Sparkleen 1 glassware detergent, acetone (Fisher Scientific, reagent grade, CAS no. 67-64-1), isopropanol (Fisher Scientific, reagent grade, CAS no. 67-63-0), ethanol, hydrogen peroxide (Fisher Scientific, CAS no. 7722-84-1), and ammonium hydroxide (Fisher Scientific, Reagent ACS grade, CAS no. 1336-21-6).

3.5.2. Reagents for Monolayers on ITO

All reagents were used as received, which included tetrahydrofuran (Calderon, HPLC grade, CAS no. 109-99-9), octadecylphosphonic acid (Sigma-Aldrich, 97%, CAS no. 4727-47-4), octadecyltrichlorosilane (Sigma-Aldrich, ≥90%, CAS no. 112-04-9), 1-octadecanol (Sigma-Aldrich, ReagentPlus® grade >99%, CAS no. 112-92-5), n-hexane (ACS, reagent grade, CAS no. 110-54-3), 1H,1H,2H,2H-perfluoro-1-octanol (Sigma-Aldrich, 97%, CAS no. 647-42-7), 1, 5-pentanediol (Sigma-Aldrich, >97%, CAS no. 111-29-5), and 1,10-decanediol (Sigma-Aldrich, 98.0%, CAS no. 112-47-0). Glass slides coated with ITO films (7 ohms cm^{-2}, polished grade, 75 × 25 × 1.1 mm with an ITO thickness of ~100 ± 10 nm) were purchased from University Wafer (Item no. 2290). The ITO coated glass slides were diced into 1 cm × 2 cm pieces. These pieces served as substrates for the following experiments. Potassium chloride (Fisher Scientific, certified ACS grade, CAS no. 7447-440-7), potassium ferricyanide (Allied Chemical, ACS reagent grade, CAS no. 1376-66-2), potassium ferrocyanide (Fisher Scientific, certified ACS grade, CAS no. 14459-95-1) were used as received without further purification.

3.5.3. Pretreatment of ITO Films on Glass Slides

Each of the cut glass slides coated with an ITO film were placed into individual glass test tubes (part no. 908035, CEM Discover). These substrates were sonicated in a detergent solution prepared from 18 MΩ·cm deionized (DI) water (10 mL, obtained from a Barnstead Nanopure Diamond water filtration system) and Sparkleen glassware detergent (1 g). The samples were sonicated sequentially in acetone, isopropanol and ethanol. The

sonication process was maintained over a period of 10 min in each solvent, and subsequently rinsed with DI water (25 mL). A modified RCA-1 cleaning procedure was performed to remove additional surface contaminants and to create hydroxyl groups on the ITO surfaces.[113] In brief, to prepare the RCA-1 cleaning solution, a glass beaker containing DI water (50 mL) was heated to 70 °C using a temperature controlled hotplate (Corning 720). Upon reading 70 °C, an aqueous solution of NH_4OH (10mL, 30% v/v) was added to the heated DI water. An aqueous solution of H_2O_2 (10 mL, 30% v/v) was subsequently added to this mixture and heated until re-equilibrating at 70 °C. The freshly prepared, hot RCA solution was transferred to the glass test tubes containing individual samples, which were held at 70 °C for 3 h. The RCA-1 solution was replaced with DI water (10 mL) and the cleaned substrates were sonicated for 10 min. The rinsed ITO substrates were dried in a drying oven (model no. 1350GM, Sheldon) maintained at 120 °C for 20 min prior to the formation of the desired monolayers.

3.5.4. Surface Modifications of ITO

3.5.4.1. Formation of Alcohol Based Self-Assembled Monolayers

A series of alcohol based monolayers were formed on the ITO surfaces. Individual clean ITO coated substrates were placed into separate 10 mL glass test tubes that contained a neat solution (~5 mL) of the desired alcohol reagent, which were heated to temperatures reaching 120 °C over a period of 24 h.

3.5.4.2. Formation of Silane Based Monolayers

A solution of ODTS was prepared in n-hexane for use in formation of monolayers on ITO following previously published techniques.[29] Individual, clean ITO coated substrates were placed into separate 10 mL glass test tubes containing the ODTS solution (~5 mL, 0.02 mM) for 2 h at room temperature.

3.5.4.3. Formation of Phosphonic Acid Based Monolayers

A solution of ODPA was prepared in tetrahydrofuran as required to make monolayers on ITO following previously published techniques.[26] Each of the ITO coated substrates were placed into individual 10 mL glass test tubes containing the ODPA solution (~0.5 mL, 0.01 mM) for up to 15 h at room temperature.

3.5.4.4. Rinsing the Prepared Substrates

Upon removal of each substrate from its corresponding preparing solution, the substrates were rinsed sequentially with ethanol (20 mL) and of DI water (200 mL). To remove any non-covalently attached molecules the substrates were sonicated in ethanol (5 mL) for 10 min. The sonicated substrates were dried under a steady stream of nitrogen gas filtered with a PTFE membrane containing <200 nm pores.

3.5.5. Characterization Procedures

The substrates were each characterized by a series of analytical techniques to assess their surface topography, hydrophobicity, chemical composition, electrochemical stability, and optical properties. Multiple measurements were obtained on each substrate to assess the surface coverage of the monolayers, as well as to assess the consistency of the coverage between each of the substrates. The parameters for each of the analytical techniques are outlined in detail below.

3.5.5.1. Cyclic Voltammetry

Cyclic voltammetry analyses were performed to investigate the electrochemical and chemical stability of the monolayers on the ITO substrates. These experiments were performed using a Biologic Potentiostat (Model SP-150) using a standard three-electrode system with a Ag/AgCl reference electrode filled with 4 M KCl (CH Instruments, part no. CHI111), a Pt counter electrode (CH Instrument, part no. CHI115) and the ITO substrates as the working electrode. The reference electrode was calibrated through measuring the electric potential difference with another standard electrode. The electrolyte solution for these experiments consisted of KCl (100 mL, 1 M) containing $K_4[Fe(CN)_6]$ (10 mM) and $K_3[Fe(CN)_6]$ (10 mM). A series of CV scans was acquired using a scan rate of 50 mV s^{-1} over a potential range from 0 to 1 V for up to 10,000 scans.

3.5.5.2. Contact Angle (CA) Measurements

The CA measurements were performed with a contact angle goniometer (Dataphysics, model OCA 15) in the Nanofabrication Facility of 4D LABS at Simon Fraser University. A droplet of DI water or hexadecane (2 μL) was dispensed onto the substrate for each of the measurements. The CA was measured as the angle between the air-water

interface of the droplet and the interface between the water and the substrate. For surface energy measurements, n-hexadecane was used in the place of water. Where applicable, error bars for the CA measurements are reported as one standard deviation from the calculated mean of eight independent measurements from a single sample.

3.5.5.3. X-ray Photoelectron Spectroscopy (XPS)

A series of XPS measurements were performed to investigate the chemical composition of the monolayers. These studies were conducted using a Kratos Analytical Axis ULTRA DLD system with a monochromatic aluminum source (Al Kα of 1486.7 eV) operating at 150 W with a 90° takeoff angle. Survey spectra (0 to 1200 eV) were acquired using a pass energy of 160 eV, a dwell time of 100 ms, and 1 sweep. High-resolution spectra were obtained using a pass energy of 20 eV, a dwell time of 500 ms, and averaging the results of 10 sweeps. This XPS analysis was performed with the assistance of a charge neutralizer because of significant charging effects from the substrates of interest. The peak positions were calibrated to the **C**-C hydrocarbon signal (C_{1s}) that was set to 285.0 eV. The peak area ratios in the high resolution XPS spectra were compared after normalization of each spectrum to the maximum signal intensity. An area of 700 μm × 300 μm was analyzed in at least three separate regions of each sample to assess the uniformity of its surface modification. Background noise was corrected through a linear fit of the baseline. Analyses and fitting of the XPS peaks was performed using Vision Processing software version 2.2.7 beta.

3.5.5.4. Ultraviolet and Visible Transmission Spectroscopy

The optical transmittance of the ITO coated substrates, acquired across the visible region of the electromagnetic spectrum, was assessed both before and after the cyclic voltammetry experiments. These spectra were obtained using an Agilent 8453 spectrophotometer. The spectral range for these studies spanned from 190 to 1100 nm with a scan time of 1.5 s. Spectral resolution of the system was set to 1.5 nm. The software package UV-Visible ChemStation Rev. A.07.01 was used to analyze these spectra.

3.5.5.5. Ultraviolet Photoelectron Spectroscopy (UPS)

A series of UPS measurements were performed to assess the work functions of the modified ITO substrates. These experiments were carried out at the University of

Washington Molecular Analysis Facility. A Kratos Axis Ultra DLD photoelectron spectrometer was used to acquire both UPS measurements and XPS survey scans. Before the UPS measurements, survey XPS spectra (0 to 1200 eV) were acquired to confirm the composition of each substrate using a monochromatic aluminum source (Al Kα of 1486.7 eV) operating with a 20 mA current at 15 kV, a pass energy of 80 eV and a data step of 1 eV. The UPS measurements used the He 1 (21.2 eV) line as the incident radiation produced from a Kratos UV lamp operating at 10 W. The UPS spectra were acquired with a pass energy of 5 eV, an aperture of 100 μm and a data step of 0.01 eV. Three independent positions on each sample were analyzed to check the uniformity of each type of surface modification. Calibration of the spectrometer was performed using a clean gold film. A 5 V battery was connected to the system to eliminate background noise. The UPS data was obtained using Casa XPS software version 2.3.15 and further processed using Vision Processing software version 2.2.7 beta.

Chapter 4.

Summary and Outlook

Despite the widespread utilization of ITO in many fields of research and in commercial products, there are still challenges of incorporating ITO into organic electronics. For example, in the case of OLED devices, multiple studies have emphasized the needs for designing the interfacial properties and chemistries of ITO to enhance the overall device performance that includes the brightness and lifetime. In this thesis work, an alternative approach to modifying the surfaces of ITO with self-assembled monolayers has been demonstrated to design interfaces with desirable work function, surface energies and stability. The results from experiments indicate alcohol based monolayers outperform the traditional procedures that utilize silanes and phosphonic acids in terms of their stabilities. Alcohol based monolayers exhibited minimal degradations in electrochemical, and chemical stabilities. The electrochemical and chemical stabilities were assessed through multiple characterization techniques, including CV, XPS, and WCA. The change in optical properties of ITO films with alcohol based monolayers were evaluated through absorption spectroscopy, namely UV-Vis transmission spectroscopy. In addition to assessing the stability of the monolayers, the work function was measured to study the electronic property.

There have been multiple approaches demonstrated in literature to address the stability and performance issues of OLED devices. The methods to characterize and evaluate the surface modifications on ITO were discussed in this thesis. These approaches include the use of metal or metal oxide thin films, and organic based monolayers. These methods have shown their effectiveness in tuning the interfacial chemistry and properties of ITO but with some limitations. The inorganic surface modifications can often have uniformity issues, where the thickness of the deposited ultrathin films is not uniform, increasing the surface roughness and adding variations to the electronic properties across this interface. This additional roughness hinders the overall performance of the device as it is limited by these localized effects. The organic surface modifications have stability issues. Monolayers prepared from both silanes and phosphonic acids, which are the common monolayers on ITO surfaces, are susceptible to

external stresses, such as hydrolytic damage and electrochemical stresses. Details on the previous achievements for the surface modifications of ITO can be found in Chapter 1. Common characterization techniques and evaluation methods used in these studies and specifically in the research introduced within this thesis were explained in detail in Chapter 2. The CV analyses were performed to assess electrochemical properties of ITO modified with monolayers and the WCA were measured to assess the change in the surface coverage and/or the degradations of the prepared monolayers after electrochemical stresses. The surface chemical composition was also pursued using XPS and investigated the changes in the species present at the surfaces before and after extensive electrochemical analyses. To further evaluate these results, an extended CV analyses either in organic solvents or use of different redox probes could be pursued on these substrates to eliminate the solvent effects. The optical properties of the prepared samples were studied using UV-Vis transmittance spectroscopy. Lastly, the electronic properties of ITO were evaluated by determining work function and surface energy.

In this thesis, alcohol based monolayers on ITO are demonstrated for the first time. This method utilizes a more affordable family of reagents, which also introduce an ease of handling and storage relative to the silanes, phosphonic acids and related species used in a number of previous studies. Monolayers derived from a series of alcohol reagents were grafted onto ITO and evaluated for their stability. The alcohol reagents used in this thesis work include simple linear alcohols, varying in their hydrocarbon chain length from 6 to 18 carbons, perfluorinated alcohols and diols. To understand and evaluate the impact of these alcohol based monolayers, an 18 hydrocarbon chain alcohol, octadecanol, was subjected to an extensive comparison with silanes and phosphonic acid monolayers derived from octadecyltrichlorosilane and octadecylphosphonic acid, respectively. The cross evaluation of these three reagents indicated that the alcohol based monolayers exhibit higher electrochemical and chemical stabilities when exposed to the same external stresses. For electronic properties, alcohol based monolayers showed a similar trend in electronic properties that has been observed for other organic monolayers in work function measurements. The work function obtained from ODA was 4.7 eV, while the work function values reported in literature for ODTS and ODPA coated ITO films were 4.85 and 4.5 eV, respectively.[27, 29] To further demonstrate work function tunability, monolayers derived from PTdiA, DCdiA and PFOA were prepared and evaluated through UPS. These reagents were chosen for their terminal function groups, hydroxyl- and perfluoro- moieties present

at the outermost surfaces of monolayers. The PFOA exhibited highest work function of 4.88 eV. The details of these studies on alcohol based monolayers are included in Chapter 3.

This thesis work focused on the assessing the characteristics of alcohol based monolayers on ITO films. Based on the findings of this work, incorporation of ITO films modified with alcohol based monolayers into OLED devices should be pursued to further evaluate their influence on device performance and lifetime. Previous studies on the performance of OLEDs used multiple strategies that include measuring quantum efficiency, luminance, and resistivity to evaluate surface modifications on ITO.[37, 39, 45, 51] One common method used to study lifetime of an OLED devices is through measuring the half-lifetime of the device. It is defined as time taken for luminance to decrease to half of its initial luminance, while maintaining a constant current.[91] These experiments will allow understanding of the difference of performance and lifetime of OLEDs utilizing alcohol based monolayer, in contrast to monolayers derived from silanes and phosphonic acids.

Another potential use of these alcohol based monolayers are in molecular sensors. Beside OLEDs and OPVs, sensors are another common type of devices that utilize ITO. In these molecular sensors, a platform that expresses diverse surface moieties at the outermost surfaces of monolayers is desired to detect various molecular species in a solution or gaseous form. Monolayers with hydroxyl terminal groups have not yet been demonstrated on ITO. Alcohol based monolayers have demonstrated this hydroxyl surface moiety at the outermost surfaces of monolayers through use of diols, which could be modified further through elimination and/or substitution of hydroxyl groups.[114-116] This new platform will enable detection of molecular species that are not currently able to be detected using sensors prepared from ITO films.

References

1.   Wu, Q.-H., Progress in Modification of Indium-Tin Oxide/Organic Interfaces for Organic Light-Emitting Diodes. *Crit. Rev. Solid State Mater. Sci.* **2013,** *38*, 318-342.

2.   Kajii, H.; Sato, Y.; Morimune, T.; Ohmori, Y., Improved Sensitivity and Durability of Poly(3-Hexylthiophene)-Based Polymeric Photodetectors Using Indium Tin Oxide Modified by Phosphonic Acid–Based Self-Assembled Monolayer Treatment. *Electron. Commun. Jpn.* **2016,** *99*, 48-53.

3.   Armstrong, N. R.; Carter, C.; Donley, C.; Simmonds, A.; Lee, P.; Brumbach, M.; Kippelen, B.; Domercyq, B.; Yoo, S., Interface Modification of ITO Thin Films: Organic Photovoltaic Cells. *Thin Solid Films* **2003,** *445*, 342-352.

4.   Rhee, S.-W.; Yun, D.-J., Metal-Semicondcutor Contact in Organic Thin Film Transistors. *J. Mater. Chem.* **2008,** *18*, 5437-5444.

5.   Lee, J.; Jung, B. J.; Lee, J. I.; Chu, H. Y.; Do, L. M.; Shim, H. K., Modification of an ITO Anode with a Hole-Transporting SAM for Improved OLED Device Characteristics. *Chem. Mater.* **2002,** *12*, 3494-3498.

6.   Sohn, S.; Kim, H.-M., *Transparecnt Conductive Oxide (TCO) Films for Organic Light Emissive Devices (OLEDs)*. InTech: 2011.

7.   Hanson, E. L.; Guo, J.; Koch, N.; Schwartz, J.; Bernasek, S. L., Advacned Surface Modification of Indium Tin Oxide for Improved Charge Injection in Organic Devices. *J. Am. Chem. Soc.* **2005,** *127*, 10058-10062.

8.   Bright, C. I., *Review of Transparent Conductive Oxide (TCO)*. Society of Vacuum Coaters: 2007.

9.   Stadler, A., Transparent Conducting Oxides - An Up-To-Date Overview. *Materials* **2012,** *5*, 661-683.

10.   Park, K.-S.; Choi, Y.-J.; Kang, J.-G.; Sung, Y.-M.; Park, J.-G., The Effect of Concentration and Oxidation State of Sn on the Sturctural Electrical Properties of Indium Tin Oxide Nanowires. *Nanotechnology* **2011,** *22*, 285712-285717.

11.   Kelin, A.; Körber, C.; Wachau, A.; Säuberlich, F.; Gassenbauer, Y.; Harvey, S. P.; Proffit, D. E.; Mason, T. O., Transparent Conducting Oxides for Photovoltaics: Manipulation of Fermi Level, Work Function and Energy Band Alignment. *Materials* **2010,** *3*, 4892-4914.

12. Paniagua, S. A.; Giordano, A. J.; Smith, O. L.; Barlow, S.; Li, H.; Armstrong, N. R.; Pemberton, J. E.; Bredas, J. L.; Ginger, D.; Marder, S. R., Phosphonic Acids for Interfacial Engineering of Transparent Conductive Oxides. *Chem. Rev.* **2016,** *116*, 7117-7158.

13. Erhart, P.; Klein, A.; Egdell, R. G.; Albe, K., Band Structure of Indium Oxide: Indirect versus Direct Band Gap. *Phys. Rev. B* **2007,** *75*, 153205.

14. Ishii, H.; Sugiyama, K.; Ito, E.; Seki, K., Energy Level Alignment and Interfacial Electronic Structures at Organic/Metal and Organic/Organic Interfaces. *Adv. Mater.* **1999,** *11* (8), 605-625.

15. Turak, A., Interfacial Degradation in Organic Optoelectronics. *RSC. Adv.* **2013,** *3*, 6188-6225.

16. Pujari, S. P.; Scheres, L.; Marcelis, A. T.; Zuilhof, H., Covalent Surface Modification of Oxide Surfaces. *Angew. Chem. Int. Ed. Engl.* **2014,** *53* (25), 6322-56.

17. Bernède, J. C.; Martinez, F.; Neculqueo, G.; Cattin, L., On the Improvement of the Electroluminescent Signal of Organic Light Emitting Diodes by the Presence of an Ultra-Thin Metal Layer at the Interface Organic/ITO. *Phys. Stat. Sol. (RRL)* **2008,** *2*, 10-12.

18. Shen, Y.; Jacobs, D. B.; Malliaras, G. G.; Koley, G.; Spencer, M. G.; Ioannidis, A., Modification of Indium Tin Oxide for Improved Hole Injection in Organic Light Emitting Diodes. *Adv. Mater.* **2001,** *13*, 1234-1238.

19. Qiu, C.; Xie, Z.; Chen, H.; Wong, M.; Kwok, H. S., Comparative Study of Metal or Oxide Capped Indium-Tin Oxide Anodes for Organic Light-Emitting Diodes. *J. Appl. Phys.* **2003,** *93*, 3253-3258.

20. Ke, L.; Kumar, R. S.; Chen, P.; Shen, L.; Chua, S.-J.; Burden, A. P., Au-ITO Anode for Efficient Polymer Light-Emitting Device Operation. *IEEE Photonics Tech. Lett.* **2005,** *17*, 543-545.

21. Chu, T.-Y.; Chen, J.-F.; Chen, S.-Y.; Chen, C.-J.; Chen, C. H., Highly Efficient and Stable inverted Bottom-Emission Organic Light Emitting Devices. *Appl. Phys. Lett.* **2006,** *89*, 053503.

22. Matsushima, T.; Kinoshita, Y.; Murata, H., Formation of Ohmic Hole Injection by Inserting an Ultrathin Layer of Molybdenum Trioxide between Indium Tin Oxide and Organic Hole-Transporting Layers. *Appl. Phys. Lett.* **2007,** *91*, 253504.

23. Lee, H.; Cho, S. W.; Han, K.; Jeon, P. E.; Whang, C.-N.; Jeong, K.; Cho, K.; Yi, Y., The Origin of the Hole Injection Improvements at Indium Tin Oxide/Molybdenum Trioxide/N,N'-bis(1-naphythyl)-N,N'-diphenyl-1,1'-biphenyl-4,4'diamine Interfaces. *Appl. Phys. Lett.* **2008,** *93*, 043308.

24. Buwen, X.; Yafeng, S.; Meng, M.; Chuannan, L., Enhancement of Hole Injection with an Ultra-Thing Ag_2O Modified Anode in Organic Light-Emitting Diodes. *Macroelectron. J.* **2005,** *36*, 105-108.

25. Hotchkiss, P. J.; Jones, S. C.; Paniagua, S. A.; Sharma, A.; Kippelen, B.; Armstrong, N. R.; Marder, S. R., The Modification of Indium Tin Oxide with Phosphonic Acids: Mechanism of Binding, Tuning of Surface Properties, and Potential for Use in Organic Electronic Applications. *Acc. Chem. Res.* **2012,** *45* (3), 337-346.

26. Koh, S. E.; McDonald, K. D.; Holt, D. H.; Dulcey, C. S.; Chaney, J. A.; Pehrsson, P. E., Phenylphosphonic Acid Functionalization of Indium Tin Xxide: Surface Chemistry and Work Functions. *Langmuir* **2006,** *22*, 6249-6255.

27. Paniagua, S. A.; Hotchkiss, P. J.; Jones, S. C.; Marder, S. R.; Mudalige, A.; Marrikar, F. S.; Pemberton, J. E.; Armstrong, N. R., Phosphonic Acid Modification of Indium-Tin Oxide Electrodes: Combined XPS/UPS/Contact Angle Studies. *J. Phys. Chem. C* **2008,** *112*, 7809-7817.

28. Paramonov, P. B.; Paniagua, S. A.; Hotchkiss, P. J.; Jones, S. C.; Armstrong, N. R.; Marder, S. R.; Brédas, J. L., Theoretical Characterization of the Indium Tin Oxide Surface and of Its Binding Sites for Adsorption of Phosphonic Acid Monolayers. *Chem. Mater.* **2008,** *2008* (20), 5131-5133.

29. Yun, D. J.; Lee, D. K.; Jeon, H. K.; Rhee, S. W., Contact Resistance between Pentacene and Indium–Tin Oxide (ITO) Electrode with Surface Treatment. *Org. Electron.* **2007,** *8*, 690-694.

30. Kim, J. S.; Park, J. H.; Lee, J. H., Control of the Electrode Work Function and Active Layer Morphology via Surface Modification of Indium Tin Oxide for High Efficiency Organic Photovoltaics. *Appl. Phys. Lett.* **2007,** *91*, 112111.

31. Kim, S. H.; Ohtsuka, H.; Advincula, R. C.; Tanaka, K., Effect of Photoreactive SAM at the Interface of an Indium-Tin Oxide Electrode and a Polymer Hole Transport Layer. *IEICE Trans. Electron.* **2013,** *96-C*, 365-368.

32. Luscombe, C. K.; Li, H. W.; Huck, W. T. S.; Holmes, A. B., Fluorinated Silane Self-Assembled Monolayers as Resists for Patterning Indium Tin Oxide. *Langmuir* **2003,** *19*, 5273-5278.

33. Bermudez, V. M.; Berry, A. D.; Kim, H.; Pique, A., Functionalization of Indium Tin Oxide. *Langmuir* **2006,** *22*, 11113-11125.

34. Hotchkiss, P. J.; Li, H.; Paramonov, P. B.; Paniagua, S. A.; Jones, S. C.; Armstrong, N. R.; Brédas, J.-L.; Marder, S. R., Modification of the Surface Properties of Indium Tin Oxide with Benzylphosphonic Acids: A Joint Experimental and Theoretical Study. *Adv. Mater.* **2009,** *21*, 4496-4501.

35.   Gardner, T. J.; Frisbie, D. C.; Wrighton, M. S., Systems for Orthogonal Self-Assembly of Electroactive Monolayers on Au and ITO: An Approach to Molecular Electronics. *J. Am. Chem. Soc.* **1995,** *117*, 6927-6933.

36.   Casalini, S.; Bortolotti, C. A.; Leonardi, F.; Biscarini, F., Self-Assembeld Monolayers in Organic Electronics. *Chem. Soc. Rev.* **2017,** *46*, 40-71.

37.   Hains, A. W.; Liu, J.; Martinson, A. B. F.; Irwin, M. D.; Marks, T. J., Anode Interfacial Tuning via Electron-Blocking/ Hole-Transport Layers and Indium Tin Oxide Surface Treatment in Bulk-Heterojunction Organic Photovoltaic Cells. *Adv. Funct. Mater.* **2010,** *20*, 595-606.

38.   Ballarin, B.; Barreca, D.; Cassani, M. C.; Carraro, G.; Maccato, C.; Mignani, A.; Lazzari, D.; Bertola, M., Fluoroalkylsilanes with Embedded Functional Groups as Building Blocks for Environmentally Safer Self-Assembled Monolayers. *Langmuir* **2015,** *31*, 6988-6994.

39.   Cui, J.; Huang, Q.; Veinot, J. G. C.; Yan, H.; Marks, T. J., Interfacial Microstructure Function in Organic Light-Emitting Diodes: Assembled Tetraaryldiamine and Copper Pthalocyanine Interlayers. *Adv. Mater.* **2002,** *14*, 565-569.

40.   Hatton, R. A.; Day, S. R.; Chesters, M. A.; Willis, M. R., Organic Electroluminescent Devices: Enhanced Carrior Injection Using an Organosilane Self Assembled Monolayer (SAM) Derivatized ITO Electrode. *Thin Solid Films* **2001,** *394*, 292-297.

41.   Bhairamadgi, N. S.; Pujari, S. P.; Trovela, F. G.; Debrassi, A.; Khamis, A. A.; Alonso, J. M.; Zaharani, A. A. A.; Wennekse, T.; Al-Turaif, H. A.; van Rijn, C.; Alhamed, Y. A.; Zuilhof, H., Hydrolytic and Thermal Stability of Organic Monolayers on Various Inorganic Substrates. *Langmuir* **2014,** *30*, 5829-5839.

42.   Marcinko, S.; Fadeev, A. Y., Hydrolytic Stability of Organic Monolayers Supported on TiO_2 and ZrO_2. *Langmuir* **2004,** *20* (6), 2270-2273.

43.   Olmos, D.; González-Benito, J.; Aznar, A. J.; Baselga, J., Hydrolytic Damage Study of the Silane Coupling Region in Coated Silica Microfibres: pH and Coating Type Effects. *J. Mater. Process. Technol.* **2003,** *143*, 82-86.

44.   Bell, M. S.; Shahraz, A.; Fichthorn, K. A.; Borhan, A., Effects of Hierarchical Surface Roughness on Droplet Contact Angle. *Langmuir* **2015,** *31*, 6752-6762.

45.   Bardecker, J. A.; Ma, H.; Kim, T.; Huang, F.; Liu, M. S.; Cheng, Y.-J.; Ting, G.; Jen, A. K.-Y., Self-Assembled Electroactive Phosphonic Acids on ITO: Maximizing Hole-Injection in Polymer Light-Emitting Diodes. *Adv. Funct. Mater.* **2008,** *18*, 3964-3971.

46. Chen, X.; Luais, E.; Darwish, N.; Ciampi, S.; Thordarson, P.; Gooding, J. J., Studies on the Effect of Solvents on Self-Assembled Monolayers Formed from Organophosphonic Acids on Indium Tin Oxide. *Langmuir* **2012,** *28*, 9487-9495.

47. Appleyard, S. F. J.; Willis, M. R., Electroluminescence: Enhanced Injection Using ITO Electrodes Coated with a Self Assembled Monolayer. *Opt. Mater.* **1998,** *9*, 120-124.

48. Angel, F. A.; Lyubarskaya, Y. L.; Shestopalov, A. A.; Tang, C. W., Degradation of Self-Assembled Monolayers in Organic Photovoltaic Devices. *Org. Electron.* **2014,** *15*, 3624-2631.

49. Habich, D. B.; Halik, M.; Schmid, G., Cyclic Voltammetry on n-Alkylphosphonic Acid Self-Assembled Monolayer Modified Large Area Indium Tin Oxide Electrodes. *Thin Solid Films* **2011,** *519*, 7809-7812.

50. Huang, Q.; Evmenenko, G. A.; Dutta, P.; Lee, P.; Armstrong, N. R.; Marks, T. J., Covalently Bound Hole-Injectiong Nanostructures. Systematics of Molecular Architecture, Thickness, Saturation, and Electron-Blocking Characteristics on Organic Light-Emitting Diode Luminance, Turn-on Voltage, and Quantum Efficiency. *J. Am. Chem. Soc.* **2005,** *127*, 10227-10242.

51. Helander, M. G.; Wang, Z. B.; Qiu, J.; Greiner, M. T.; Puzzo, D. P.; Liu, Z. W.; Lu, Z. H., Chlorinated Indium Tin Oxide Electrodes with High Work Function for Organic Device Compatibility. *Science* **2011,** *332*, 944-947.

52. Huang, L.; Chen, L.; Huang, P.; Wu, F.; Tan, L.; Xiao, S.; Zhong, W.; Sun, L.; Chen, Y., Triple Dipole Effect from Self-Assembled Small-Molecules for High Performance Organic Photovoltaics. *Adv. Mater.* **2016,** *28*, 4852-4860.

53. Lee, A. W.; Gates, B. D., Rapid Covalent Modification of Silicon Oxide Surfaces through Microwave-Assisted Reactions with Alcohols. *Langmuir* **2016,** *32*, 7284-7293.

54. Hackett, N. G.; Zangmeister, C. D.; Hacker, C. A.; Richter, L. J.; Richter, C. A., Demosntration of Molecular Assembly on Si (100) for CMOS-Compatible Molecule-Based Electronic Devices. *J. Am. Chem. Soc.* **2008,** *130*, 4259-4261.

55. Cleland, G.; Horrocks, B. R.; Houlton, A., Direct Functionalization of Silicon via the Self-Assembly of Alcohols. *J. Chem. Soc. Faraday Trans.* **1995,** *91*, 4001-4003.

56. Boukherroub, R.; Morin, S.; Sharpe, P.; Wayner, D. D. M., Insights into the Formation Mechanisms of Si-OR Monolayers from the Thermal Reactions of Alcohols and Aldehydes with Si(111)-H. *Langmuir* **2000,** *16*, 7429-7434.

57.   Szwajca, A.; Krzywiecki, M.; Koroniak, H., Self-Assembled Monolayers of Partially Fluorinated Alcohols on Si (0 0 1): XPS and UV-Photoemission Study. *J. Fluorine Chem.* **2015,** *180*, 248-256.

58.   Aguiar, F. A.; Campos, R.; Wang, C.; Jitchati, R.; Batsanov, A. S.; Bryce, M. R.; Kataky, R., Comparative Electrochemical and Impedance Studies of Self-Assembled Rigid-Rod Molecular Wires and Alkanethiols on Gold Substrates. *Phys. Chem. Chem. Phys.* **2010,** *12*, 14804-14811.

59.   *Colloid Science: Principles, Methods and Applications*. Blackwell Publishing Ltd: Oxford, Britain, 2005.

60.   Baghbanzadeh, M.; Simeone, F. C.; Bowers, C. M.; Liao, K. C.; Thuo, M.; Baghbanzadeh, M.; Miller, M. S.; Carmichael, T. B.; Whitesides, G. M., Odd-Even Effects in Charge Transport across n-alkanethiolate-Based SAMs. *J. Am. Chem. Soc.* **2014,** *136*, 16919-16925.

61.   Liu, Y.-F.; Lee, Y.-L., Adsorption Characteristics of OH-Terminated Alkanethiol and Arenethiol on Au (111) Surfaces. *Nanoscale* **2012,** *4*, 2093-2100.

62.   Muthurasu, A.; Ganesh, V., Electrochemical Characterization of Self-Assembled Monolayers (SAMs) of Silanes on Indium Tin Oxide (ITO) Electrodes-Tuning Electron Transfer Nehaviour across Electrode-Electrolyte Interface. *J. Colloid Interface Sci.* **2012,** *374*, 241-249.

63.   Ganesh, V.; Pal, S. K.; Kumar, S.; Lakshminarayanan, V., Self-Assembled Monolayers (SAMs) of Alkoxycyanobiphenyl Thiols on Gold - A Study of Electron Transfer Reaction Using Cyclic Voltammetry and Electrochemical Impedance Spectroscopy. *J. Colloid Interface Sci.* **2006,** *296*, 195-203.

64.   Reiger, P. H., *Electrochemistry*. Springer Science+Business Media Dordrecht: 1994.

65.   Connelly, N. G.; Geiger, W. E., Chemical Redox Agents for Organometallic Chemistry. *Chem. Rev.* **1996,** *96*, 877-910.

66.   Brett, C. M. A.; Brett, A. M. O., *Electrochemsitry Principles, Methods and Applications*. Oxford: New York, 1993.

67.   Mabbott, G. A., An Introduction to Cyclic Voltammetry. *J. Chem. Educ.* **1983,** *60*, 697-702.

68.   Kissinger, P. T.; Heineman, W. R., Cyclic Voltammetry. *J. Chem. Educ.* **1983,** *60*, 702-706.

69.   Nicholson, R. S., Theory and Application of Cyclic Voltammetry for Measurements of Electrode Reaction Kinetics. *Anal. Chem.* **1965,** *37*, 1351-1355.

70.   García-Raya, D.; Madueño, R.; Sevilla, J. M.; Blázquez, M.; Pineda, T., Electrochemical Characterization of a 1,8-Octanedithiol Self-Assembled Monolayers (ODT-SAM) on a AU (1 1 1) Single Crystal Electrode. *Electrochim. Acta* **2008,** *53*, 8026-8033.

71.   Martinez, L.; Leinen, D.; Martín, F.; Gabas, M.; Ramos-Barrado, J. R.; Quagliata, E.; Dalchiele, E. A., Electrochemical Growth of Diverse Iron Oxide (Fe3O4, - FeOOH, and -FeOOH) Thin Films by Electrodeposition Potential Tuning. *J. Electrochem. Soc.* **2007,** *154*, D126-D133.

72.   Rock, P. A., The Standard Oxidation Potential of the Ferrocyanide-Ferricyanide Electrode at 25° and the Entropy of Ferrocyanide Ion. *J. Phys. Chem.* **1966,** *70*, 576-580.

73.   Żenkiewicz, M., Methods for the Calculation of Surface Free Energy of Solids. *J. Achiev. Mater. Manuf. Eng.* **2007,** *24*, 137-145.

74.   Owens, D. K.; Wendt, R. C., Estimation of the Surface Free Energy of Polymers. *J. Appl. Polym. Sci.* **1969,** *13*, 1741-1747.

75.   *Surface and Thin Film Analysis: A Compendium of Principles, Instrumentation and Applications*. 2nd ed.; Wiley-VCH Verlag & Co. KGaA: Weinheim, Germany, 2011.

76.   Hofmann, S., *Auger- and X-Ray Photoelectron Spectroscopy in Materials Science*. Springer Series in Surface Science 2013.

77.   Börgel, J.; Campbell, M. G.; Ritter, T., Transition Metal d-Orbital Splitting Diagrams: An Updated Educational Resource for Square Planar Transition Metal Complexes. *J. Chem. Educ.* **2016,** *93*, 118-121.

78.   Rocha, A. B., Spin-Orbit Splitting for Inner-Shell 2p States. *J. Mol. Model* **2014,** *20*, 2355.

79.   Leckey, R., *Ultraviolet Photoelectron Spectroscopy of Solids*. 2nd ed.; Springer: Berlin, 2003.

80.   Ishii, H.; Kudo, K.; Nakayama, T.; Ueno, N., *Electronic Processes in Organic Electronics*. Springer: Tokyo, Japan, 2015.

81.   Kahn, A., Fermi Level, Work Function and Vacuum Level. *Mater. Horiz.* **2016,** *3*, 7-10.

82.   Bredas, J.-L., Mind the Gap! *Mater. Horiz.* **2014,** *1*, 17-19.

83.   Braun, S.; Salaneck, W. R.; Fahlman, M., Energy-Level Alignment at Organic/Metal and Organic/Organic Interfaces. *Adv. Mater.* **2009,** *21*, 1450-1472.

84.   Donley, C.; Dunphy, D.; Paine, D.; Carter, C.; Nebesny, K.; Lee, P.; Alloway, D.; Armstrong, N. R., Characterization of Indium-Tin Oxide Interfaces Using X-ray Photoelectron Spectroscopy and Redox Processes of a Chemisorbed Probe Molecule: Effect of Surface Pretreatment Conditions. *Langmuir* **2001,** *18*, 450-457.

85.   Choi, M.; Jo, K.; Yang, H., Effect of Different Pretreatments on Indium-Tin Oxide Electrodes. *Bull. Korean Chem. Soc.* **2013,** *34*, 421-425.

86.   M.;, C.; Havare, A. K.; Aydin, H.; Yagmurcukardes, N.; Demic, S.; Icli, S.; Okur, S., Electrical Properties of SAM-modified ITO Surface Using Aromatic Small Molecules with Double Bond Carboxylic Acid Groups for OLED Applications. *Appl. Surf. Sci.* **2014,** *314*, 1082-1086.

87.   Yeh, M. C.; Kramer, E. J.; Sharma, R.; Zhao, W.; Rafailovich, M. H.; Sokolov, J.; Brock, J. D., Thermal Stability of Self-Assembled Monolayers from Alkylchlorosilanes. *Langmuir* **1996,** *12*, 2747-2755.

88.   Azia, H.; Popovic, Z. D.; Hu, N. X.; Hor, A. M.; Xu, G., Degradation Mechanism of Small Molecule-Based Organic Light-Emitting Devices. *Science* **1999,** *283*, 1900-1902.

89.   You, Z. Z.; Dong, J. Y., Surface Properties of Treated ITO Anodes for Organic Light-Emitting Devices. *Appl. Surf. Sci.* **2005,** *249*, 271-276.

90.   Burrows, P. E.; Bulovic, V.; Forrest, S. R.; Sapochack, L. S.; McCarty, D. M.; Thompson, M. E., Reliability and Degradation of Organic Light Emitting Devices. *Appl. Phys. Lett.* **1994,** *65*, 2922-2924.

91.   Yu, S. Y.; Chang, J. H.; Wang, P. S.; Wu, C. I.; Tao, Y. T., Effect of ITO Srface Modification on the OLED Device Lifetime. *Langmuir* **2014,** *30*, 7369-7376.

92.   Pfeiffer, K.; Shestaeva, S.; Bingel, A.; Munzert, P.; Ghazaryan, L.; Helvoirt, C. V.; Kessels, W. M. M.; Sanli, U. T.; Grévent, C.; Schütz, G.; Putkonen, M.; Buchanan, I.; Jensen, L.; Ristau, D.; Tünnermann, A.; Szeghalmi, A., Comparative Study of ALD SiO_2 Thin Films for Optical Applications. *Opt. Mater. Express* **2016,** *6*, 660-670.

93.   Linfor, M. R.; Chidsey, C. E. D., Alkyl Monolayers Covalently Bonded to Silicon Surfaces. *J. Am. Chem. Soc.* **1993,** *115*, 12631-12632.

94.   Zhu, X.-Y.; Boiadjiev, V.; Mulder, J. A.; Hsung, R. P.; Major, R. C., Molecular Assemblies on Silicon Surfaces via Si-O Linkages. *Langmuir* **2000,** *16*, 6766-6772.

95.   Major, R. C.; Zhu, X.-Y., Two-Step Approach to the Formation of Organic Monolayers on the Silicon Oxide Surface. *Langmuir* **2001,** *17* (18), 5576-5580.

96.   Li, J.; Ji, S.; Zhang, G.; Guo, H., Surface-Modification of Poly(dimethylsiloxane) Membrane with Self-Assembled Monolayers for Alcohol Permselective Pervaporation. *Langmuir* **2013,** *29*, 8093-8102.

97.   Finklea, H. O.; Avery, S.; Lynch, M., Blocking Oriented Monolayers of Alkyl Mercaptans on Gold Electrodes. *Langmuir* **1987,** *3*, 409-413.

98.   Millone, M. A.; Hamoudi, H.; Rodriguez, L.; Rubert, A.; Benitez, G. A.; Vela, M. E.; Salvarezza, R. C.; Gayone, J. E.; Sanchez, E. A.; Grizzi, O.; Dablemont, C.; Esaulov, V. A., Self-Assembly of Alkanedithiols on Au(111) from Solution: Effect of Chain Length and Self-Assembly Conditions. *Langmuir* **2009,** *25*, 12945-12953.

99.   Shepherd, J. L.; Bizzotto, D., Characterization of Mixed Alcohol Monolayers Adsorbed onto a Au(111) Electrode Using Electro-Fluorescence Microscopy. *Langmuir* **2006,** *22*, 4869-4876.

100.   Wang, W.; Dibenedetto, A. T., A Modified Silane Treatment for Superior Hydrolytic Stability of Glass Reinforced Composites. *J. Adhesion* **1998,** *68*, 183-201.

101.   Cotterll, T. L., *The Strengths of Chemical Bonds*. 2nd ed.; Butterworths Scientific Publications: London, 1954.

102.   Maeng, M.; Kim, J.-H.; Hong, J.-A.; Park, Y., Effects of Oxygen Plasma Treatments on the Work Function of Indium Tin Oxide Studied by in-situ Photoelectron Spectroscopy. *J. Korean Phys. Soc.* **2016,** *68*, 692-696.

103.   Mutin, P. H.; Guerrero, G.; Vioux, A., Hybrid Materials from Organophosphorous Coupling Molecules. *J. Mater. Chem.* **2005,** *15*, 3761-3768.

104.   Tsai, T.; Wu, Y., Wet Etching Mechanisms of ITO Films in Oxalic Acid. *Mircroelectron. Eng.* **2006,** *83*, 536-541.

105.   Swain, B.; Mishra, C.; Hong, H. S.; Cho, S. S.; Lee, S. K., Commercial Process for the Recovery of Metals from ITO Etching Industry Wastewater by Liquid-Liquid Extraction: Simulation, Analysis of Mechanism, and Mathematical Model to Predict Optimum Operational Conditions. *Green Chem.* **2015,** *17*, 3979-3991.

106.   Li, M.-C.; Wan, D.-S.; Lee, C.-C., Application of White-Light Scanning Interferometer on Transparent Thin-Film Measurements. *Appl. Opt.* **2012,** *51* (

), 8579-8586.

107.   Custódio, J. V.; Agostinho, S. M. L.; Simões, A. M. P., Electrochemistry and Surface Analysis of the Effect of Benzotriazole on the Cut Edge Corrosion of Galvanized Steel. *Electrochim. Acta* **2010,** *55*, 5523-5531.

108.	Schlaf, R.; Murata, H.; Kafafi, Z. H., Work Function Measurements on Indium Tin Oxide FIlms. *J. Electron. Spectrosc. Relat. Phenom.* **2001,** *120*, 149-154.

109.	Kim, J. S.; Lägel, B.; Moons, E.; Johansson, N.; Baikie, I. D.; Salaneck, W. R.; Friend, R. H.; Cacialli, F., Kelvin Probe and Ultraviolet Photoemission Measurements of Indium Tin Oxide Work Function: a Comparison. *Synth. Met.* **2000,** *111*, 311-314.

110.	Yuan, L.; Thompson, D.; Cao, L.; Nerngchangnong, N.; Nijhuis, C. A., One Carbon Matters: the Origin and Reversal of Odd-Even Effects in Molecular Diodes with SAMs of Ferrocenyl-Alkanethiolates. *J. Phys. Chem. C* **2015,** *119*, 17910-17919.

111.	Porter, M. D.; Bright, T. B.; Allara, D. L.; Chidsey, C. E. D., Spontaneously Organized Molecular Assemblies. 4. Structural Characterization of n-Alkyl Thiol Monolayers on Gold by Optical Ellipsometry, Infrared Spectroscopy, and Electrochemistry. *J. Am. Chem. Soc.* **1987,** *109*, 3559-3568.

112.	Yildirim, O.; Yilmaz, M. D.; Reinhoudt, D. N.; Blank, D. H. A.; Rijnders, G.; Huskens, J., Electrochemical Stability of Self-Assembled Alkylphosphate Monolayers on Conducting Metal Oxides. *Langmuir* **2011,** *27*, 9890-9894.

113.	Kern, W., The Evolution of Silicon Wafer Cleaning Technology. *J. Electrochem. Soc.* **1990,** *137*, 1887-1892.

114.	Brunrit, A.; Dahlstrand, C.; Olsson, S. K.; Srifa, P.; Huang, G.; Orthaber, A.; Sjöberg, P. J. R.; Biswas, S.; Himo, F.; Samec, J. S. M., Brøsted Acid-Catalyzed Intramolecular Nucleophilic Substituion of the Hydroxyl Group in Stereogenic Alcohols with Chirality Transfer. *J. Am. Chem. Soc.* **2015,** *137*, 4646-4649.

115.	Dabbagh, H. A.; Salehi, J. M., New Transition-State Models and Kinetics of Elimination Reactions of Tertiary Alcohols over Aluminum Oxide. *J. Org. Chem.* **1998,** *63*, 7619-7627.

116.	Bunrit, A.; Dahlstrand, C.; Srifa, P.; Olsson, S. K.; Huang, G.; Biswas, S.; Himo, F.; Samec, J. S. M., Nucleophilic Substitution of the Hydroxyl Group in Stereogenic Alcohols with Chirality Transfer. *Synlett* **2016,** *27*, 173-176.

Appendix A.

Three-Electrode Setup

The standard setup for the three-electrode setup used in this thsis for CV analyses is shown in Figure A1. This experiment was performed on a bench top without controlling the environment. Three holes were drilled on the lid for RE, CE, and WE.
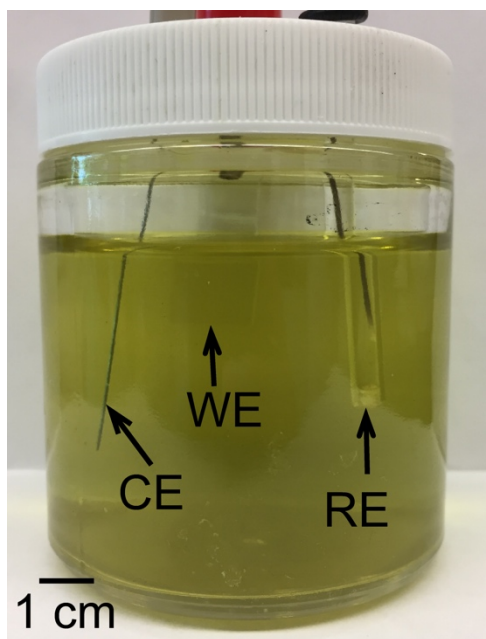

Figure A1. Three-electrode setup used for cyclic voltammetry (CV). WE = working electrode (ITO), CE = counter electrode (Pt wire) and RE = reference electrode (Ag/AgCl electrode)

Appendix B.

X-ray Photoelectron Survey Scans and High Resolution Scans of ITO Films Modified with Monolayers

All of the typical XPS survey scans for monolayers on ITO included in this thesis are shown in this appendix. Figure B1 depicts the XPS survey scan of clean native ITO. The typical XPS survey scans of ODA, ODTS and ODPA coated ITO substrates before and after electrochemical tests are shown in Figure B2 to B7. In addition, XPS survey scans of PTdiA, DCdiA and PFOA coated ITO substrates are also included in this section, as well as their high resolution O_{1s} scans (Figure B8 to B13).
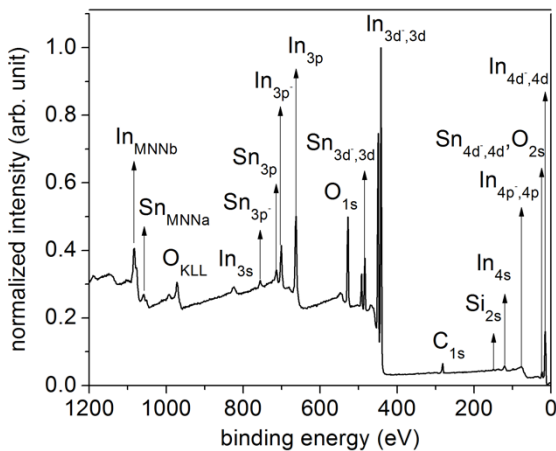
Figure B1. A typical XPS survey scan of an RCA-1 cleaned ITO substrate.
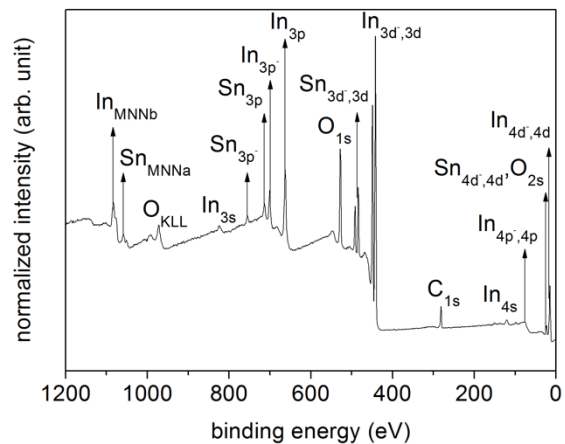
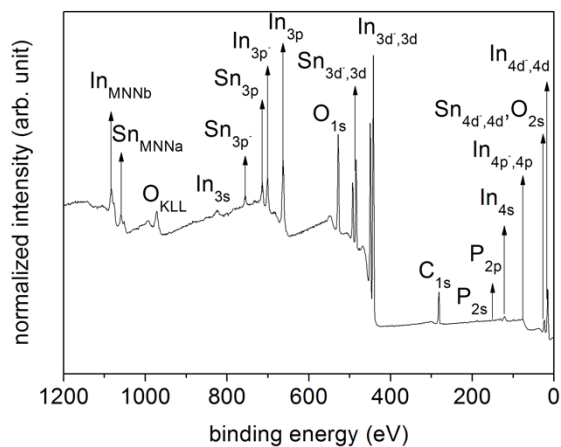**Figure B2.** A typical XPS survey scan of the ODA coated ITO substrates.
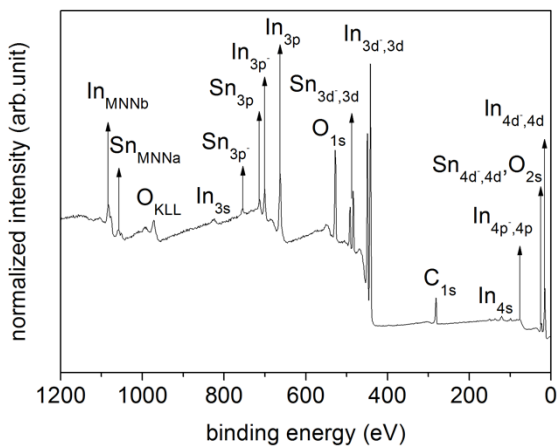
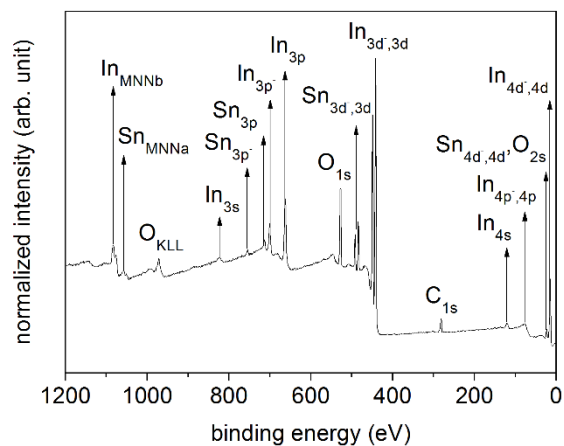**Figure B3.** A typical XPS survey scan for ODA coated ITO after extensive electrochemical and hydrolytic tests.
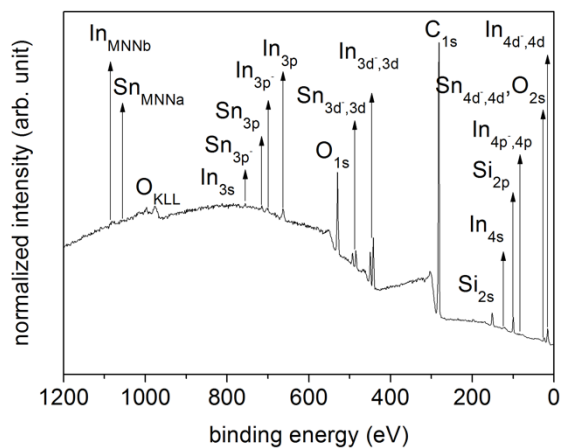
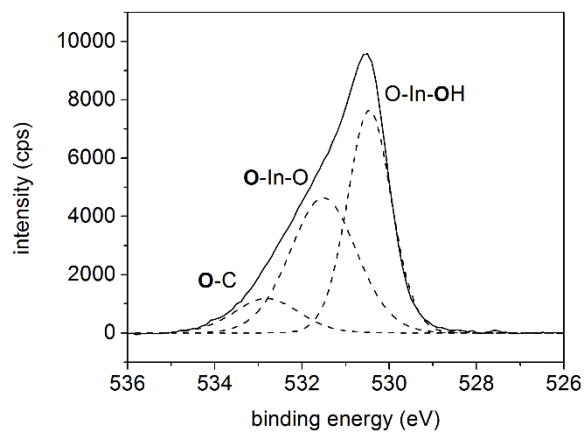**Figure B4.** A typical XPS survey scan of the ODTS coated ITO substrate.
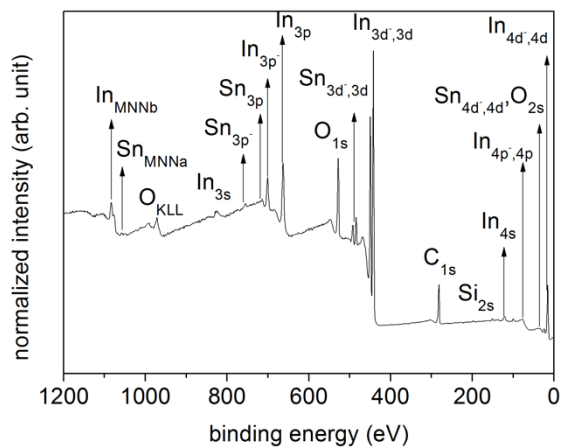
Figure B5. A typical XPS survey scan of the ODTS coated ITO after extensive electrochemical and hydrolytic tests.
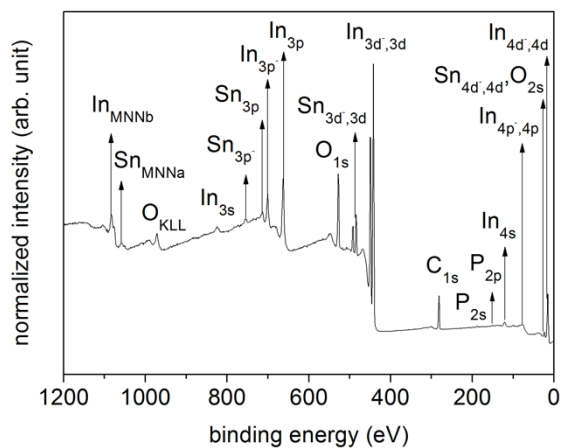
Figure B6. A typical XPS survey scan of the ODPA coated ITO substrates.

Figure B7. A typical XPS survey scan of the ODPA coated ITO after extensive electrochemical and hydrolytic tests.

Figure B8. A typical XPS survey scan of the PTdiA coated ITO.

Figure B9. High resolution XPS scan of the O_{1s} species in DCdiA based monolayers on ITO.
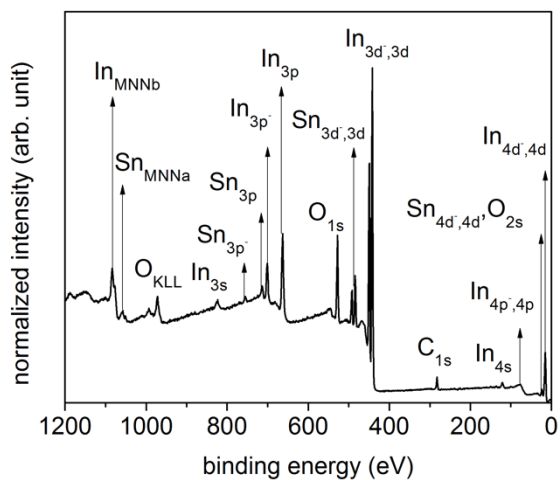
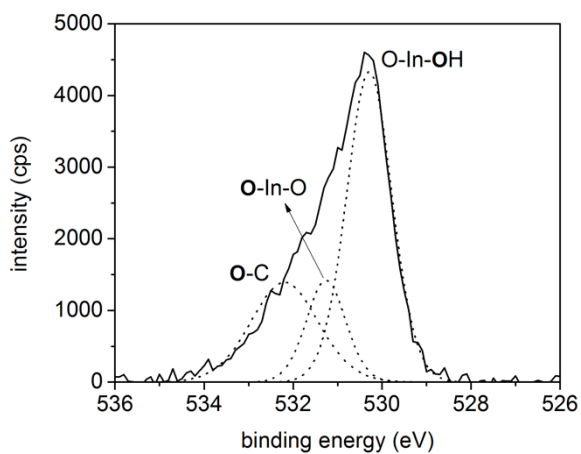**Figure B10.** A typical XPS survey scan of the DCdiA coated ITO.

Figure B11. High resolution XPS scan of the O_{1s} species in DCdiA based monolayers on ITO.

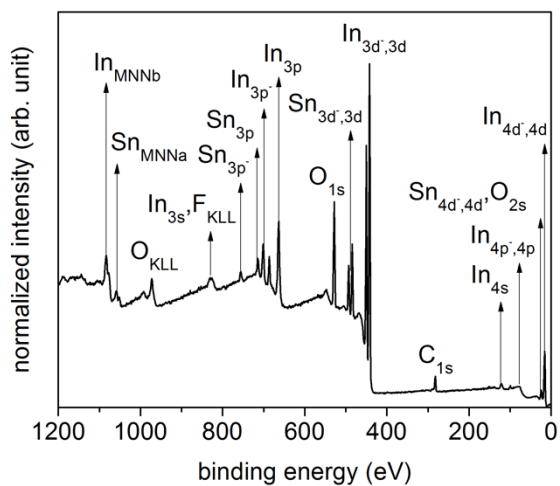**Figure B12.** A typical XPS survey scan of PFOA coated ITO.
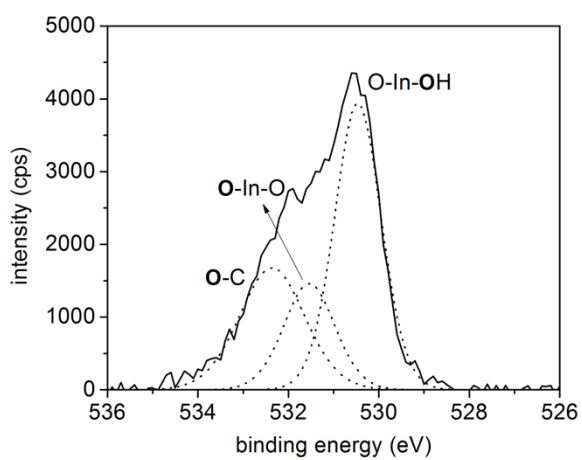

Figure B13. High resolution XPS scan of the O_{1s} species in PFOA based monolayers on ITO.